Fermi gas with attractive potential and spin $S = \frac{3}{2}$ in a one-dimensional trap: Response functions for superfluidity and FFLO signatures

P. Schlottmann[1] and A. A. Zvyagin[2,3]

[1]*Department of Physics, Florida State University, Tallahassee, Florida 32306*

[2]*B.I. Verkin Institute for Low Temperature Physics and Engineering, Ukrainian National Academy of Sciences, 47 Lenin Avenue, Kharkov, 61103, Ukraine*

[3]*Max-Planck-Institut für Physik komplexer Systeme, D-01187, Dresden, Germany*

(Received 23 December 2011; revised manuscript received 21 April 2012; published 18 May 2012)

In the context of a gas of ultracold atoms with effective spin $S = 3/2$ confined to an elongated trap, we study the one-dimensional Fermi gas interacting via an attractive δ-function potential within the grand-canonical ensemble. The particles can be either unbound or clustered in bound states of two, three, and four fermions. The rich μ versus H ground-state phase diagram (μ is the chemical potential and H the external magnetic field) consists of the four basic states and the various possible mixed phases in which some these states coexist. Extending the analysis of K. Yang [Phys. Rev. B **63**, 140511(R) (2001)] for $S = 1/2$, we study the correlation functions of the generalized Cooper clusters of bound states of two, three, and four particles using conformal field theory and the exact Bethe *Ansatz* solution. The correlation functions consist of a power law with distance times a sinusoidal term oscillating with distance. In an array of tubes with weak Josephson tunneling, the type of superfluid order is determined by these correlation functions. The wavelength of the oscillations is related to the periodicity of a generalized Fulde-Ferrell-Larkin-Ovchinnikov (FFLO) state for higher spin particles. All the relevant states are analyzed for $S = 3/2$.

DOI: 10.1103/PhysRevB.85.205129 PACS number(s): 71.10.Pm, 36.40.Ei, 51.30.+i

I. INTRODUCTION

Spin-imbalanced ultracold gases of atoms confined to one-dimensional traps have been the subject of several recent studies.[1–3] Confinement to nearly one-dimensional tubes can be achieved if the ultracold cloud of atoms is subjected to a two-dimensional optical lattice, which defines a two-dimensional array of tubes.[1] The tubes can be regarded as isolated if the confinement by the laser beams is strong enough to suppress tunneling between tubes. The scattering between atoms under transverse harmonic confinement is subject to a confinement-induced resonance.[4] Fine tuning this Feshbach-type resonance, the interaction between the fermions can be made attractive and its strength can be varied.[5] The interaction is local and can be approximated by a δ-function potential in space. The confinement along the tube is roughly harmonic and weak; it can be locally incorporated into the chemical potential. Consequently, these systems of fermions are only locally homogeneous and within the local density approximation display phase separation with the variation of the chemical potential along the tube.[2,3] Although most experimental findings so far are for ^{6}Li atoms (spin $1/2$),[1,6–8] recent results for ^{40}K (spin $9/2$) are very encouraging that soon higher spins will be investigated.[9]

One-dimensional spin-$1/2$ gases with δ-function interaction were first studied by M. Gaudin[10] and C. N. Yang[11] extending Bethe's *Ansatz*. For an attractive interaction in the ground state there are two classes of solutions of the discrete Bethe *Ansatz* equations, namely, real charge rapidities and paired complex conjugated rapidities,[10,12,13] representing spin-polarized particles and bound states of the Cooper type, respectively. There are then three possible homogeneous phases, namely, the (1) fully spin-polarized state, (2) a phase without polarization, where all particles are bound in Cooper pairs, and (3) a mixed phase in which unpaired spin-polarized particles coexist with Cooper pairs. In phase (2), the Cooper pairs are gapped (i.e., it requires a critical field to break-up the bound states) and display no long-range order. Similar results were obtained for the Hubbard model with attractive U.[14,15] There are several other theoretical studies, Refs. 16–28, of ultracold spin-$1/2$ atoms in one dimension, which are related to the present work.

Sutherland[29] generalized the Bethe *Ansatz* solution for spin $1/2$ to an arbitrary number of colors $N = 2S + 1$ [SU(N) symmetry]. For an attractive interaction, Takahashi[30] derived the integral equations for the ground-state density functions for bound states of up to $N = 2S + 1$ particles. The space extension of these bound states was further studied by C. H. Gu and C. N. Yang.[31] The classification of states, the thermodynamics, the ground-state equations and elementary excitations of the gas arbitrary number of colors have been derived by Schlottmann[32,33] for both attractive and repulsive potential (see also Ref. 34). Several of these results have been recently rederived in the context of ultracold fermion gases.[35–38] With an attractive interaction, atoms with spin S can form bound states of up to $(2S + 1)$ particles, extending this way the concept of Cooper pairs to larger clusters, and the phase diagram will have more possible pure and mixed phases.[36,39] For instance, for $S = 3/2$, there are four basic states, namely, bound states of four, three, and two particles, and unbound particles, and the corresponding mixed phases, which can have up to four coexisting basic states.

A two-body interaction for spin larger than $1/2$ does not necessarily have to have SU(N) symmetry as it is assumed here. Spin-$3/2$ fermion models with contact interactions in any dimension display a generic SO(5) symmetry without tuning parameters.[40] The Hubbard variant for $S = 3/2$ has been studied via Monte Carlo algorithms in Ref. 41 and was applied to investigate the competing orders in one-dimensional

optical traps in Ref. 42. Several integrable one-dimensional continuum models displaying pairing involving exchange interactions,[43] SO(5) symmetry for spin-3/2 fermions,[44] and hidden Sp(2s + 1) and SO(2s + 1) symmetries for high spin-s fermions and bosons[45] have been constructed and solved for the low particle density limit. Experimental results on high spin atomic gases will have to decide which model is the appropriate one.

The mixed phase for $S = 1/2$ has been interpreted[21] as the one-dimensional analog of the FFLO state.[46] For an isolated tube there is no long-range order of the pairs and hence no order parameter; however, the Cooper-pair correlation function acquires a phase in the mixed state, that is believed to be reminiscent of the space modulation of the order parameter in higher dimensions. A coupling between tubes, e.g., Josephson tunneling, increases the effective dimension of the system so that long-range order can arise and it is believed that this could lead to the realization of the FFLO phase in an ultracold gas of atoms.[1,21] The crossover from three-dimensional (FFLO phase) to one-dimensional (mixed phase) behavior is addressed in Ref. 47, where the phase diagram for a weakly interacting array of tubes is calculated. FFLO related phases have been observed in the strongly anisotropic heavy-electron compound[48,49] $CeCoIn_5$ (the interpretation is still controversial[50]) and in the quasi-two-dimensional organic compounds λ-$(BETS)_2FeCl_4$ and $(TMTSF)_2ClO_4$.[51,52]

Motivated by the work of K. Yang[21] in this paper we explore the possible formation of FFLO states in the mixed phases of quasi-one-dimensional systems with particles of spin S larger than 1/2. As a concrete example, we will work with $S = 3/2$, but the results can be extended to other spin values. For $S = 3/2$ bound states of two, three, and four particles occur which, as Josephson tunneling between tubes is allowed, may give rise to long-range superfluid order. The instability from the normal phase to the first superfluid phase is determined by the dominant one-dimensional correlation function. In a mixed phase, since the Fermi momenta for the different spin-components are different due to the magnetic field, the order parameters will have sinusoidal oscillations in space, characteristic of an FFLO state. In the one-dimensional case, the periods of oscillation can be extracted from the corresponding correlation functions. We evaluate the response functions using conformal field theory and the Bethe *Ansatz* solution. The correlation functions are the product of a power-law dependence of the distance and a cosine term with the desired periodicity. There are numerous correlation functions and the critical exponent can be used to determine which one yields the dominant behavior.

The rest of the paper is organized as follows. We start with the simplest situation: $S = 1/2$ particles. In Sec. II, we present the model and the discrete Bethe *Ansatz* equations for $S = 1/2$ and evaluate the Cooper-pair correlation function in the paired particle phase and the mixed phase using conformal field theory, thus reproducing K. Yang's[21] bosonization results. In Sec. III, we present the Bethe *Ansatz* equations and their numerical solution for the dressed energies and the densities for the case $S = 3/2$. The phase diagram for a Zeeman splitting and the phase separation due to the varying chemical potential along the trap are reviewed.[39] In Sec. IV, we turn to the correlation functions for $S = 3/2$. The matrix of dressed generalized charges is calculated and standard conformal field theory is applied to calculate the correlation functions. Results for the correlation functions as a function of the chemical potential for $H = c^2$ and $H = 2c^2$ are presented in Sec. V. The conclusions are summarized in Sec. VI.

II. BETHE *ANSATZ* EQUATIONS AND PAIRING CORRELATION FUNCTION FOR SPIN-1/2 PARTICLES

A. Model and Bethe *Ansatz*

The Hamiltonian for a gas of nonrelativistic particles with spin $S = 1/2$ interacting via an attractive δ-function potential is

$$\mathcal{H} = -\sum_{i=1}^{N_p} \frac{\partial^2}{\partial x_i^2} - 2|c| \sum_{i<j} \delta(x_i - x_j), \tag{1}$$

where x_i are the coordinates of the particles, N_p is the total number of particles and c is the interaction strength. Here, $\hbar^2/2m$, where m is the mass of the particles, has been equated to 1, or alternatively it has been scaled into $\mathcal{H}$ and c. The model is integrable and a solution can be constructed by nesting two Bethe *Ansätze* in terms of two sets of rapidities, one for the particles (charges), $\{k_j\}$, $j = 1, \ldots, N_p$, and one for the spin degrees of freedom, $\{\lambda_\alpha\}$, $\alpha = 1, \ldots, M$, where M is the number of minority spins.[10,11] With periodic boundary conditions on a ring of length L this gives rise to the discrete Bethe *Ansatz* equations.

For an attractive interaction and large L, the solutions of the Bethe equations for the ground state can be classified according to (i) $N_p - 2M$ real charge rapidities, belonging to the set $\{k_j\}$, representing unpaired propagating particles, and (ii) M pairs of complex conjugated charge rapidities associated with a spin rapidity λ_α, in the form $k_\pm = \lambda \pm |c|/2$. These pairs correspond to bound states of particles with different spin components, so-called strings of length one.[10,12,32,34] The real rapidities k_j and λ_α have all to be different and satisfy the Fermi-Dirac statistics, i.e., the states are either occupied or empty. In the ground state, the rapidities are densely distributed in the interval $[-B_l, B_l]$, where $l = 0$ and 1 is the length of the string. We denote with $\varepsilon^{(0)}(k)$ and $\varepsilon^{(1)}(\lambda)$ the energy potentials (entering the Fermi-Dirac distribution), which satisfy the following coupled linear integral equations:[12,32,34]

$$\varepsilon^{(0)}(k) = k^2 - \mu - H/2 - \int_{-B_1}^{B_1} d\lambda \varepsilon^{(1)}(\lambda) a_1(k - \lambda), \tag{2}$$

$$\varepsilon^{(1)}(\lambda) = 2\lambda^2 - c^2/2 - 2\mu - \int_{-B_0}^{B_0} dk \varepsilon^{(0)}(k) a_1(\lambda - k) - \int_{-B_1}^{B_1} d\lambda' \varepsilon^{(1)}(\lambda') a_2(\lambda - \lambda'), \tag{3}$$

where

$$a_n(x) = \frac{1}{\pi} \frac{n|c|/2}{x^2 + n^2c^2/4}, \tag{4}$$

μ is the chemical potential for the total number of particles and H is the Zeeman energy. μ and H correspond to the Langrange multipliers for the conservation of particles and the magnetization, respectively. They determine the integration limits B_l through the condition that $\varepsilon^{(l)}(\pm B_l) = 0$, since

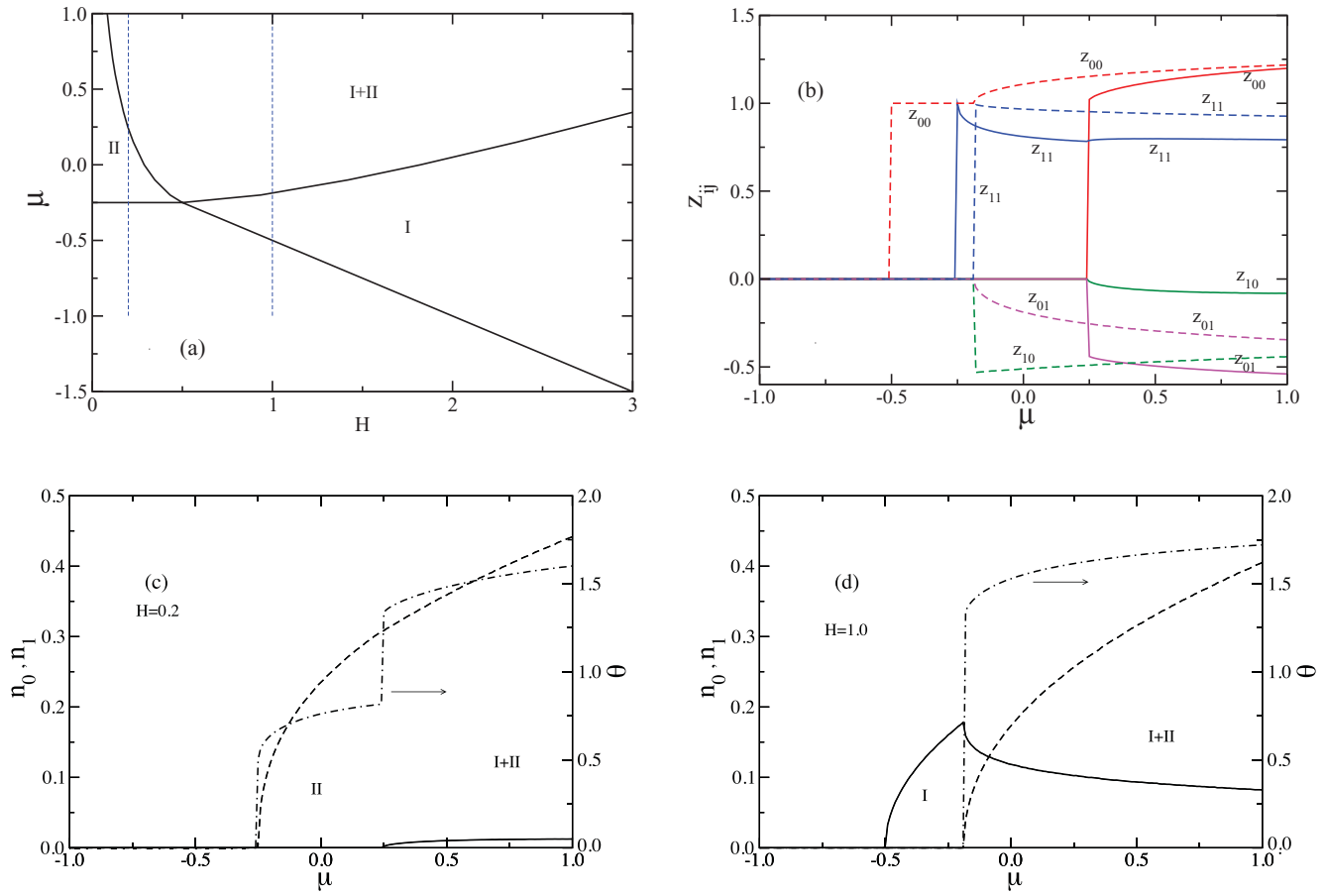

FIG. 1. (Color online) (a) Ground-state phase diagram μ vs H for a homogeneous fermion gas of spin $S = 1/2$ with $|c| = 1$.[2] The lower left corner corresponds to the empty system (no particles). The roman number I denotes unpaired particles and II denotes paired bound states. The region I + II corresponds to the mixed phase with coexisting phases I and II. The two vertical lines at $H = 0.2$ and 1.0 are μ intervals considered in the remaining panels. (b) Dressed generalized charges for the gas as a function of μ along the vertical lines $H = 0.2$ (solid curves) and $H = 1.0$ (dashed curves). (c) Occupation numbers n_0 of unpaired particles (solid), n_1 of bound pairs (dashed), and the exponent θ of the Cooper pair correlation function (dash-dotted, right axis) as a function of μ for $H = 0.2$. (d) Same as (c) but for $H = 1.0$.

occupied states correspond to $\varepsilon^{(l)} < 0$ and for empty states, $\varepsilon^{(l)}$ is positive. This way the B_l play the role of Fermi points for the spin-polarized states and the Cooper pairs, respectively.

Note that if all the $\varepsilon^{(l)}$ are rescaled to $\varepsilon^{(l)}/c^2$, μ to μ/c^2, H to H/c^2, both B_l to $B_l/|c|$, k to $k/|c|$, and λ to $\lambda/|c|$, the equations are universal, i.e., independent of the magnitude of $|c|$. The problem has then only two parameters, namely, H and μ.[2] In other words, by fixing μ and H the total number of particles and the spin polarization are determined. The phase diagram, obtained by numerically solving Eqs. (2) and (3), is shown in Fig. 1(a) and agrees with published results.[2] There are three possible phases, namely, a phase where all particles are paired denoted with II (the rapidity band $l = 1$ is partially populated and the band $l = 0$ is empty), a phase where all particles are unpaired and spin-polarized denoted with I (the rapidity band $l = 0$ is partially populated and the band $l = 1$ is empty), and the mixed phase I + II where pairs coexist with unpaired spin-polarized particles. The pure phase II is only stable for small Zeeman splitting. The harmonic confinement of the trap can be treated within the local density approximation and incorporated into the chemical potential μ.[1–3,39] μ is largest at the center of the trap and decreases as one moves away from the center towards the boundaries [see Sec. III, Eq. (27)]. In a constant magnetic field, this corresponds to a vertical line in Fig. 1(a). The two dashed vertical lines represent two qualitatively different situations of varying particle density, in which one moves from the mixed phase at the center of the trap into a pure phase, namely, phase II at low fields and phase I at higher fields, respectively. Hence, phase separation is expected as a function of the position along the trap.[2] We will refer to these transitions later in this section.

B. Distribution densities of rapidities

The distribution densities of the rapidities, $\rho^{(0)}(k)$ and $\rho^{(1)}(\lambda)$, can be obtained via differentiation of the potentials $\varepsilon^{(l)}$ with respect to the chemical potential μ,

$$\rho_h^{(0)}(k) + \rho^{(0)}(k) = -\frac{1}{2\pi}\frac{\partial\varepsilon^{(0)}(k)}{\partial\mu},$$
$$\rho_h^{(1)}(\lambda) + \rho^{(1)}(\lambda) = -\frac{1}{2\pi}\frac{\partial\varepsilon^{(1)}(\lambda)}{\partial\mu}, \tag{5}$$

where $\rho_h^{(l)}$ is the corresponding distribution density of the holes (unoccupied states). The density functions satisfy the

following integral equations:[12]

$$\rho_h^{(0)}(k)+\rho^{(0)}(k)=\frac{1}{2\pi}-\int_{-B_1}^{B_1}d\lambda\rho^{(1)}(\lambda)a_1(k-\lambda), \quad (6)$$

$$\rho_h^{(1)}(\lambda)+\rho^{(1)}(\lambda)=\frac{1}{\pi}-\int_{-B_0}^{B_0}dk\rho^{(0)}(k)a_1(\lambda-k) -\int_{-B_1}^{B_1}d\lambda'\rho^{(1)}(\lambda')a_2(\lambda-\lambda'). \quad (7)$$

The density of unpaired polarized particles and the density of paired states are given by[12]

$$n_0=\int_{-B_0}^{B_0}dk\rho^{(0)}(k), \quad n_1=\int_{-B_1}^{B_1}d\lambda\rho^{(1)}(\lambda)\,, \quad (8)$$

and the total number of particles and the magnetization per unit length are $N_p/L=n_0+2n_1$ and Magnetization$/L=n_0/2$. n_0 and n_1 as a function of the chemical potential at constant magnetic field are shown in Figs. 1(c) and 1(d) for the two situations corresponding to the vertical dashed lines in Fig. 1(a), respectively. In Fig. 1(c), it is seen that with decreasing μ there is a transition from the mixed phase (n_0 and n_1 are both nonzero) to the phase II (only n_1 is nonzero). At the boundary, n_0 vanishes with a square-root dependence, while variation of n_1 is smooth. In Fig. 1(d), we observe that with decreasing μ the transition is from the mixed phase to the spin-polarized phase I. In the mixed phase, both n_0 and n_1 are nonzero and n_1 vanishes with a square-root dependence at the phase boundary, while n_0 has a cusp at that point.

The total energy of the system is given by[12]

$$E_{\rm GS}=L\epsilon_\infty=\int_{-B_0}^{B_0}dkk^2\rho^{(0)}(k) +2\int_{-B_1}^{B_1}d\lambda(\lambda^2-c^2/4)\rho^{(1)}(\lambda), \quad (9)$$

where ϵ_∞ is the energy density. If a band is partially filled, the group velocity for the band is defined as[33]

$$v_l=\left(\frac{d\varepsilon^{(l)}(\xi)}{d\xi}\Big|_{\xi=B_l}\right)\Big/[2\pi\rho^{(l)}(B_l)], \quad (10)$$

where ξ is either k or λ. Here v_0 is the group velocity for the low-lying spin excitations and v_1 the one for the low-lying excitations of the paired bound states. In the mixed phase, both excitation states form a simple Dirac sea with two Fermi points at $\xi=\pm B_l$. The respective Fermi momenta are $p_l=\pi n_l$.

C. Conformal towers

The low-lying excitations of the system with periodic boundary conditions can be described by the finite-size corrections to the ground-state energy:[53–55]

$$E=L\epsilon_\infty+\sum_{l=0,1}\frac{\pi v_l}{2L}\left[\sum_{q=0,1}(\hat{z}^{-1})_{lq}\Delta N_q\right]^2 +\sum_{l=0,1}\frac{2\pi v_l}{L}\left\{\left[\sum_{q=0,1}z_{ql}D_q\right]^2+n_l^+ +n_l^- -\frac{1}{12}\right\}, \quad (11)$$

and the corresponding momentum is

$$\Delta P=\frac{2\pi}{L}\sum_{l=0,1}(D_l\Delta N_l+n_l^+-n_l^-)\,. \quad (12)$$

Here, z_{ql} is the 2×2 matrix of generalized dressed charges and ΔN_q, D_q, and $n_q^\pm$ are a set of eight quantum numbers characterizing the excitations. The generalized dressed charges determine how the different Fermi points (there are four) interact with each other. The dressed generalized charges are obtained as $z_{lq}=\xi_{lq}(B_q)$, where the ξ_{lq} is the solution of a set of integral equations analogous to that satisfied by the distribution densities, Eqs. (6) and (7), but with different driving terms,

$$\xi_{l0}(\lambda)=\delta_{l,0}-\int_{-B_1}^{B_1}d\lambda'\xi_{l1}(\lambda')a_1(\lambda-\lambda'),$$

$$\xi_{l1}(\lambda)=\delta_{l,1}-\int_{-B_0}^{B_0}d\lambda'\xi_{l0}(\lambda')a_1(\lambda-\lambda') -\int_{-B_1}^{B_1}d\lambda'\xi_{l1}(\lambda')a_2(\lambda-\lambda'). \quad (13)$$

Figure 1(b) shows the dressed generalized charges as a function of the chemical potential at constant magnetic field for the two situations corresponding to the vertical dashed lines in Fig. 1(a). The solid lines refer to the $H=0.2$ case, while the dashed curves represent the $H=1.0$ case. In the mixed phase, both bands are occupied and hence all four dressed generalized charges are different from zero. This changes in the pure phases, where only one rapidity band is populated and hence the dressed generalized charge is a scalar, corresponding to z_{ll} for that band. The off-diagonal dressed charges are negative in the mixed phase, while the diagonal components are positive. Their variation at the transitions can also be discontinuous, which reflects in jumps of the critical exponent (see below). The dressed generalized charges for the Tonks-Girardeau limit were obtained in Ref. 28.

The eight quantum numbers consist of two sets of four quantum numbers, one for each band of rapidities. ΔN_q corresponds to the added or removed number of particles in the rapidity band q, D_q is the parity variable, i.e., $2D_q$ is the difference between forward and backward movers in the band q, and the $n_q^\pm$ count the number of particle and hole excitations about each Fermi point (+ for forward movers and − for backward movers). These eight quantum numbers determine the conformal asymptote of the correlation function for a given conformal field operator $\mathcal{O}$. At $T=0$, the corresponding space and time-dependent correlation function is given by[53–55]

$$\langle\mathcal{O}^\dagger(x,t)\mathcal{O}(0,0)\rangle=\frac{\exp[-2i(D_0p_0+D_1p_1)x]}{\prod_{l=0,1}(x-iv_lt)^{2\Delta_l^+}(x+iv_lt)^{2\Delta_l^-}}, \quad (14)$$

where p_l are the Fermi momenta and $\Delta_l^\pm$ are the conformal dimensions defined as

$$2\Delta_0^\pm=2n_0^\pm+\left[z_{00}D_0+z_{10}D_1\pm\frac{z_{11}\Delta N_0-z_{01}\Delta N_1}{2(z_{00}z_{11}-z_{10}z_{01})}\right]^2,$$

$$2\Delta_1^\pm=2n_1^\pm+\left[z_{01}D_0+z_{11}D_1\mp\frac{z_{10}\Delta N_0-z_{00}\Delta N_1}{2(z_{00}z_{11}-z_{10}z_{01})}\right]^2. \quad (15)$$

The smallest exponents are obtained for $n_0^\pm=n_1^\pm=0$.

The backward scattering quantum numbers, D_q, are actually related to the ΔN_q via the discrete Bethe *Ansatz* equations, i.e., the equations before the thermodynamic limit is taken. Removing or adding a pair of particles (or and unpaired particle) rearranges the quantum numbers of the rapidities yielding the following relations:[28]

$$D_0 = \tfrac{1}{2}(\Delta N_0 + \Delta N_1) \pmod 1, \quad D_1 = \tfrac{1}{2}\Delta N_0 \pmod 1. \tag{16}$$

Hence, depending on ΔN_0 and ΔN_1, D_0 and D_1 can be integers or half integers, but they are only determined modulo an integer.

In recent papers,[56–59] it was shown that neglecting irrelevant operators perturbing the Luttinger-liquid Hamiltonian can lead to incorrect results for on-shell singularities in correlation functions. Introducing a coupling to a mobile impurity and taking the leading irrelevant operators into account nonperturbatively, it is possible to recover the exact singularity threshold and critical exponent. We do, however, believe that these irrelevant operators do not affect the exponent of the equal-time correlation functions studied here.

D. Cooper pair correlation function and FFLO phase

For simplicity, we restrict ourselves to the equal-time correlation function for the Cooper pairs. Denoting the creation of a Cooper pair by $C_p^\dagger$, the corresponding correlation function has the following general form:

$$\langle C_p^\dagger(x,0)C_p(0,0)\rangle = Ax^{-\theta}\ \exp[-2i(D_0 p_0 + D_1 p_1)x]\ , \tag{17}$$

where

$$\theta = 2(\Delta_0^+ + \Delta_0^- + \Delta_1^+ + \Delta_1^-) \tag{18}$$

and A is an amplitude.

We first consider the pure phase II for which we only have to consider two quantum numbers, namely, ΔN_1 and D_1. The addition of a bound pair of particles corresponds to $\Delta N_1 = 1$ and from Eq. (16) we have that D_1 is an integer. In terms of particle creation operators, the operator associated with $D_1 = 0$ is $c^\dagger_{1/2+}c^\dagger_{-1/2-}$, where the subscripts refer to the spin component and $+/-$ to forward/backward movers. This represents a standard Cooper pair, which is a bound state of a forward moving spin-up particle with a backward moving spin-down particle, and has zero total spin and momentum. Another possible choice is $D_1 = 1$, which corresponds to the operator $c^\dagger_{1/2+}c^\dagger_{-1/2+}$ and carries momentum $2\pi n_1 D_1$, but is different from a Cooper pair. The above arguments correspond to a system with periodic boundary conditions, although the trap is actually open ended (see Ref. 39). However, transport quantities should be calculated with periodic boundary conditions, since the possibility of a current circulating should exist. For $\Delta N_1 = 1$, $D_1 = 0$, and $n_1^\pm = 0$ (the leading contribution involves no particle-hole excitations about the Fermi points), we obtain $\theta = 1/(2z_{11}^2)$ and $\langle C_p^\dagger(x,0)C_p(0,0)\rangle = Ax^{-\theta}$,[54] in agreement with results obtained using the bosonization method.[21]

We now consider the mixed phase, where both rapidity bands are populated. The quantum numbers for the band of pairs are not changed, $\Delta N_1 = 1$, $D_1 = 0$, and $n_1^\pm = 0$. The band for spin-polarized unpaired particles has $\Delta N_0 = 0$ (the number of unpaired particles is not changed) and from Eq. (16) it is seen that the parity of the states is changed by the addition of a Cooper pair, $D_0 = \pm 1/2$ and $n_0^\pm = 0$ for the smallest conformal dimensions. When inserted into Eq. (15), we obtain for the critical exponent,

$$\theta = \frac{1}{2}\left(z_{01}^2 + z_{00}^2\right)\left[1 + \frac{1}{(z_{11}z_{00} - z_{10}z_{01})^2}\right], \tag{19}$$

and the correlation function is given by

$$\langle C_p^\dagger(x,0)C_p(0,0)\rangle = Ax^{-\theta}\ \cos(\pi n_0 x), \tag{20}$$

where we neglected an arbitrary constant phase in the cosine function. The period of oscillation has been obtained in Sec. II B [see Figs. 1(c) and 1(d)] and θ is shown as the dash-dotted curve in the same panels (right side axis). Note that θ is discontinuous at the transition between phases. θ is in qualitative agreement with the result obtained through the bosonization method.[21] The critical scaling dimension in one-dimension is 2, and $\theta < 2$ is satisfied for both, the II and the I + II, phases in the region of interest. The correlation function for the Tonks-Girardeau limit was also obtained in Ref. 28.

Next, we consider an array of parallel elongated tubes. The tubes are assumed to be all equal. The particles in different tubes interact with each other and a weak tunneling of unpaired and preformed pairs of particles between tubes is allowed. The Josephson tunneling leads to coherence between the pairs in different tubes and eventually to long-range order of Cooper pairs that propagate along the direction of the tubes. If the system is in phase II, the long-range order is the condensation of pairs of up-spin right movers with down-spin left movers, as expected from the BCS theory, only that the Fermi surface is one-dimensional with Fermi momentum $k_F = \pi n_1$.[21] The three-dimensional order gives rise to a low but finite T_c, and for T above T_c the Luttinger liquid power-law behavior of the Cooper-pair correlation function (17) remains valid. This power law determines the onset of superfluidity from the normal phase. The situation is more complicated in the mixed I + II phase, since the Fermi momenta for up-spin and down-spin are different, namely, $k_{F\uparrow} = \pi(n_0 + n_1)$ and $k_{F\downarrow} = \pi n_1$, respectively. It is then straightforward to see that with transversal coherence the BCS theory yields momentum carrying Cooper pairs and the order parameter is an oscillating function of space, in complete analogy with the FFLO phase.[21] The space modulation of the order parameter is just given by the oscillating factor in Eq. (20). The phase is then not homogeneous, but due to the nodes of the order parameter, there are periodically alternating regions of BCS condensate and normal phases.

E. Density wave correlation functions

Particle density waves and spin density waves are two other possible forms of long-range order that can be considered. The correlation function for longitudinal (along the z axis) spin density waves is very similar to that of particle density waves, so that we can refer to them as density waves. In terms of creation and annihilation operators, the local density operator

for up-spin particles is

$$\psi_\uparrow^\dagger(x)\psi_\uparrow(x) = \frac{1}{L}\sum_{k,k'}(c_{k\uparrow+}^\dagger e^{ik_\uparrow x} + c_{k\uparrow-}^\dagger e^{-ik_\uparrow x}) \times (c_{k'\uparrow+}e^{-ik_\uparrow x} + c_{k'\uparrow-}e^{ik_\uparrow x}), \quad (21)$$

and a similar expression holds for down-spin particles. None of the operators changes the number of particles, so that $\Delta N_0 = \Delta N_1 = 0$ for all of them. Consequently, the parity operators are integers. Operators with both fermion operators referring to the same Fermi point have $D_0 = D_1 = 0$, while a momentum transfer of $\pm 2k_\uparrow$ correspond to $D_0 = D_1 = \pm 1$ and of $\pm 2k_\downarrow$ to $D_0 = 0$ and $D_1 = \pm 1$. The critical exponents are computed from the conformal dimensions, Eq. (15). The terms with $D_0 = D_1 = 0$ yield a constant term given by the square of the particle density (square of the magnetization) for the particle density (spin density) correlation function. The terms with nonzero D quantum numbers give rise to nontrivial results. The density correlation function for the Tonks-Girardeau limit was also obtained in Ref. 28.

For the pure phase II (all particles are paired), only z_{11} matters and the density wave exponent is $\theta_{\rm DW} = 2z_{11}^2$, which is the inverse of the exponent for superfluidity. z_{11} is close to one for small particle density and hence superfluidity is favored. With increasing μ, z_{11} decreases and at some critical value of μ for which $z_{11} = 1/\sqrt{2}$, the two exponents are equal to one. For larger particle populations, the density waves are favored.

In a finite magnetic field H and with increasing μ, the system eventually crosses over into the mixed phase. When entering the mixed phase the exponent for superfluidity increases dramatically, as seen in Figs. 1(c) and 1(d). $\theta_{\rm DW}$, on the other hand, decreases considerably because $z_{11} > 0$ and $z_{00} > 0$ but z_{10} and z_{01} are both negative. Under these circumstances, the density waves dominate and one could expect a coexistence of three types of order in the ground state, namely, ferromagnetism, particle density waves, and spin density waves. There are two different wave numbers of oscillation, which are $(2\pi n_\uparrow)$ and $(2\pi n_\downarrow)$ and the exponents for both spin directions are different in the mixed phase. Let us assume that the order is governed by the spin direction with the smaller exponent; then there is a modulation either for the up-spins or the down-spins, but not for both. If the up-spins are modulated, both paired and unpaired particles are modulated and hence the down-spins are also modulated. On the other hand, if the modulation is for down-spins, then, since the particles are bound, the up-spins are also modulated. In other words, both, up- and down-spin particle densities, have to be modulated simultaneously, but since the Fermi vectors are different the periodicities are going to be different.

In order to generate long-range order at finite temperatures, the transversal coherence among a large number of tubes is required. This can be obtained by tunneling of Cooper pairs between tubes induced by constructing the optical lattice so that the tubes are not perfectly isolated. The tunneling of particles between tubes also smears the build-up of density waves, which this way become unfavorable. We therefore limit ourselves to study superfluidity response functions for the remainder of this paper. Symmetry breaking due to the tunneling of pairs between two chains has been studied in Ref. 60 in the context of the Coulomb drag between quantum wires.

Finally, there is a third operator that could be relevant for density waves, $c_{\uparrow+}^\dagger c_{\uparrow-} c_{\downarrow-}^\dagger c_{\downarrow+}$, i.e., an up-spin particle jumps forward and a down-spin particle backward across the Fermi surface. The only nonzero quantum number is then $D_0 = \pm 1$. This term yields oscillations with a wave number of $(2\pi n_0)$, but the corresponding exponent θ is larger than 2 (larger than the critical scaling dimension) and hence this operator is not relevant.

III. GENERALIZATION TO SPIN-3/2 PARTICLES

For $S > 1/2$, the model under consideration is still given by Eq. (1) only that the internal spin symmetry is now SU(N) with $N = 2S + 1$. The corresponding Bethe *Ansatz* equations have been derived by Sutherland.[29,34] For an attractive interaction and large L, the solutions of the discrete Bethe equations for the ground state are strings of length of up to $N - 1$. We denote the rapidities with $\xi^{(l)}$, where $l = 0, \ldots, N - 1 = 2S$. For $S = 3/2$, there are then four sets of states, namely, $\xi^{(3)}$, corresponding to bound states of four particles, $\xi^{(2)}$, referring to bound states of three particles, $\xi^{(1)}$, representing bound pairs, and $\xi^{(0)}$ for the unbound spin-polarized particles.[30,33,34] This classification of states is completely analogous to that of the Anderson impurity of arbitrary spin in the $U \to \infty$ limit[61] (see also Refs. 62–64, and 66) and the one-dimensional degenerate supersymmetric t-J model,[65] and is only determined by the SU(N) symmetry and the attractive nature of the potential.

The real rapidities $\xi^{(l)}$ have all to be different and satisfy the Fermi-Dirac statistics, i.e., the states are either occupied or empty. In the ground state, the rapidities are densely distributed in the interval $[-B_l, B_l]$. We denote with $\varepsilon^{(l)}(\xi)$, $l = 0, 1, \ldots, 2S$, the dressed energy potentials (entering the Fermi-Dirac distribution) and with $\rho^{(l)}(\xi)$ the densities of the rapidities. These quantities satisfy integral equations that generically for a quantity $X^{(l)}$ for $l = 0, \ldots, 2S$ can be written as

$$X^{(l)}(\xi) = D_l(\xi) - \sum_{q=0}^{2S}\int_{-B_q}^{B_q} d\xi' K_{lq}(\xi - \xi')X^{(q)}(\xi'), \quad (22)$$

where $D_l(\xi)$ is the driving term and $K_{lq}(\xi)$ the integration kernel. The kernel can be written in a compact form:[33]

$$K_{lq}(\xi) = \int \frac{d\omega}{2\pi} \exp[i\xi\omega - (l + q - p_{l,q})|\omega c|/2] \times \sinh[(p_{l,q} + 1)\omega c/2]/\sinh(\omega c/2), \quad (23)$$

where $p_{l,q} = \min(l, q) - \delta_{l,q}$. Note that $K_{lq}(\xi) = K_{ql}(\xi)$. In terms of the $a_n(\xi)$ defined in Eq. (4), the kernel for $S = 3/2$ is

$$\begin{aligned} &K_{00} = 0, \quad K_{01} = a_1, \quad K_{02} = a_2, \quad K_{03} = a_3, \\ &K_{11} = a_2, \quad K_{12} = a_1 + a_3, \quad K_{13} = a_2 + a_4, \\ &K_{22} = a_2 + a_4, \quad K_{23} = a_1 + a_3 + a_5, \quad K_{33} = a_2 + a_4 + a_6. \end{aligned} \quad (24)$$

The four dressed energy potentials for a Zeeman splitting are obtained from Eq. (22) with the driving terms[33,34]

$$D_l(\xi) = (l + 1)\left[\xi^2 - \frac{l(l + 2)}{12}c^2 - \mu - \frac{3 - l}{2}H\right]. \quad (25)$$

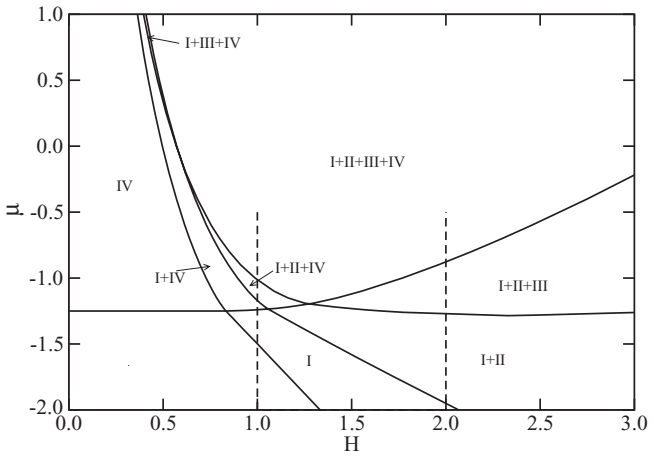

FIG. 2. Ground-state phase diagram μ vs H for a homogeneous fermion gas of spin $S = 3/2$ with $|c| = 1$.[39] The roman numbers denote the number of particles involved in a bound state. Regions with more than one roman number are mixed phases, i.e., phases with coexisting different states. The lower left corner corresponds to the empty system, i.e., no particles. The two vertical dashed lines at constant field, $H = 1.0$ and 2.0 are μ intervals considered in Figs. 4 and 5 to discuss phase separation along the trap.

The Lagrange multipliers μ and H determine the integration limits B_l through the condition that $\varepsilon^{(l)}(\pm B_l) = 0$, in analogy to the $S = 1/2$ case. This determines the Fermi points of the system. Note that if all the $\varepsilon^{(l)}$ are rescaled to $\varepsilon^{(l)}/c^2$, μ to μ/c^2, H to H/c^2, all B_l to $B_l/|c|$, and ξ to $\xi/|c|$, the equations are universal, i.e., independent of the magnitude of $|c|$. Hence, within the framework of the grand canonical ensemble, without loss of generality, it is sufficient to present the results for $|c| = 1$. The phase diagram has then only two parameters, namely, H and μ. The above set of equations is solved numerically by iteration and the phase diagram for $|c| = 1$ is shown in Fig. 2. The energy potential $\varepsilon^{(0)}$ corresponds to unpaired particles with spin-component $S_z = 3/2$; the energy $\varepsilon^{(1)}$ to bound pairs with spin-components $S_z = 3/2$ and $S_z = 1/2$; the potential $\varepsilon^{(2)}$ to bound states of three particles of spin components $S_z = 3/2$, $S_z = 1/2$, and $S_z = -1/2$, respectively; and finally, $\varepsilon^{(3)}$ to bound states of four particles all with different spin components. We denote these states with roman numbers, I, II, III, and IV, respectively. These states can coexist in mixed phases, for example we denote with I + IV the coexistence of unpaired and bound states of four particles and with I + II + III a phase where all states except four-particle bound states are present.[39]

Note that all phase boundaries are given by the zero of some energy potential. The phase boundaries are then crossover lines, which are accompanied by a square-root singularity of one of the densities of states (one-dimensional van Hove singularity, see inset of Fig. 4 of Ref. 39). For small magnetic fields all particles are bound in four-particle bound states (generalized Cooper pairs). The lower left corner refers to the region where all bands are empty (system without particles). With increasing field other phases become realized. At very large magnetic fields and/or for low values of μ (small number of particles) the phase IV is not favorable. For large μ and intermediate magnetic fields, all four bands are populated and hence spin-polarized unbound particles coexist with all possible bound states.

An ultracold atom gas is inherently inhomogeneous since the diameter of the tube gradually changes with position from the center of the trap to its boundaries. As a consequence of the changing diameter of the tube, the quantization in the plane transversal to the tube gradually changes the zero of energy. This change can be represented by a harmonic potential, so that the actual local chemical potential μ is a function of x given by

$$\mu(x) + \tfrac{1}{2} m\omega_{ho}^2 x^2 = \text{const.} \tag{26}$$

Within the local density approximation, it is $\mu(x)$ that enters the Bethe equations for $\varepsilon^{(l)}$. The solution is then exact for the one-dimensional system, but approximative for the trap. This approximation[1–3] is expected to be good since the variation of μ with x is slow, i.e., it is the largest length scale in the system. The approximation neglects the quantization of the harmonic confinement, which is treated classically and locally incorporated into the chemical potential. Given $\mu(0)$ and $\mu(L/2)$, i.e., the chemical potential at the center and boundary of the trap, the position along the trap is given by [from Eq. (26)]

$$x/(L/2) = \sqrt{[\mu(x) - \mu(0)]/[\mu(L/2) - \mu(0)]}\,. \tag{27}$$

The two dashed vertical lines in Fig. 2 represent two very different situations for the variation with μ in a constant magnetic field.

In order to obtain the local density profile as a function of x for the different phases, the density functions for the rapidities have to be computed. The density functions of the rapidities are obtained from the dressed energies $\varepsilon^{(q)}(\xi)$ by differentiation with respect to μ,[33,34]

$$\rho_h^{(q)}(\xi) + \rho^{(q)}(\xi) = -\frac{1}{2\pi}\frac{\partial \varepsilon^{(q)}(\xi)}{\partial \mu}, \tag{28}$$

where $\rho^{(q)}(\xi)$ is the particle density and $\rho_h^{(q)}(\xi)$ the corresponding hole density for bound states involving $q + 1$ particles. The integral equations satisfied by the density functions are of the form of Eq. (22) with $X^{(l)}(\xi) = \rho_h^{(q)}(\xi) + \rho^{(q)}(\xi)$ and $D_l(\xi) = (l + 1)/(2\pi)$.[30] After solving these equations numerically, the density of bound states in each class is given by

$$n_q = \int_{-B_q}^{B_q} d\xi \rho^{(q)}(\xi)\,. \tag{29}$$

The local density profiles as a function of x [with x given by Eq. (27)] for the different phases for $H = 1.0$ and 2.0 are displayed in Fig. 3. These cases correspond to the vertical dashed lines in Fig. 2. The thin vertical lines in Fig. 3 indicate the transitions between the phases. The solid lines represent the density of four-particle bound states, the dashed curves the density of three-particle bound states, the dotted lines the concentration of pairs, and the dash-dotted curves the density of unpaired polarized particles. As a function of x the system then displays phase separation. Note that the densities vanish with a square-root singularity that is characteristic of one-dimensional van Hove singularities[39] as seen in Fig. 3. The total density of particles, $N_p/L = \sum_{q=0}^{3}(q + 1)n_q$, is shown as the blue curves in Fig. 3. The magnetization density

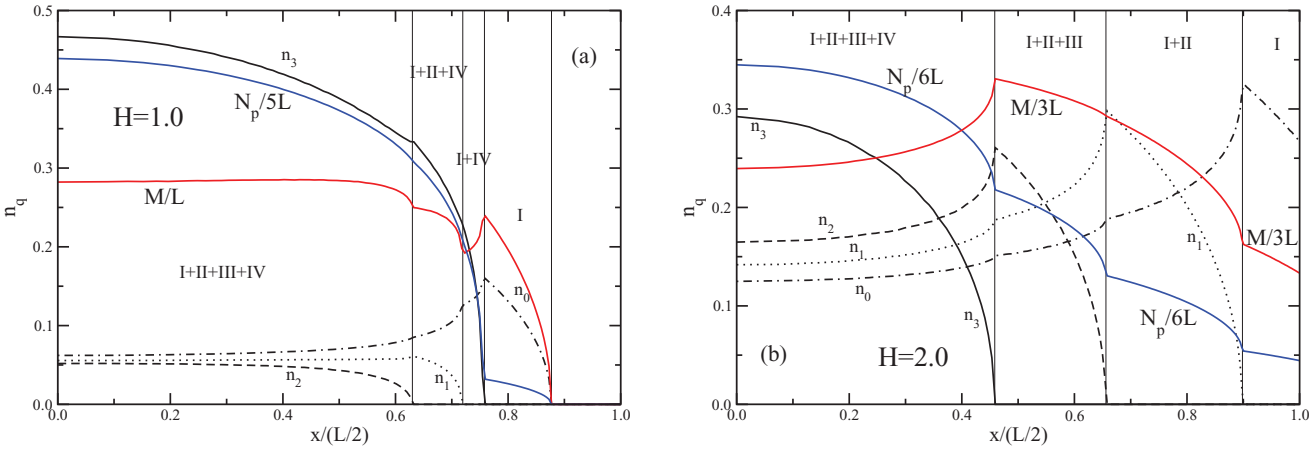

FIG. 3. (Color online) Density profile within the local density approximation for $|c| = 1$, $S = 3/2$ and (a) $H = 1.0$ [$\mu(0) = -0.5$ and $\mu(L/2) = -1.8$] and (b) $H = 2.0$ [$\mu(0) = -0.5$ and $\mu(L/2) = -2.3$]. The position along the trap is given by Eq. (27). The four (three) crossovers between phases are shown by the thin vertical lines. The densities n_q of bound states of $q+1$ particles (or polarized unbound particles if $q = 0$) are given by the solid (n_3), dashed (n_2), dotted (n_1), and dash-dotted (n_0) curves. There is phase separation due to the varying confinement along the trap.[39] The solid blue curve represents the density of the total number of particles, N_p/L, rescaled by a factor of 5 [in (a) and 6 in (b)], respectively. The red curve is the magnetization density, M/L [rescaled by a factor of 3 in (b)].

$M/L = \sum_{q=0}^{3}(q+1)(3-q)n_q/2$ is represented by the red curves in Fig. 3. Note the rescaling factors for both, the total particle density and the magnetization density.

IV. CONFORMAL TOWERS AND SUPERFLUIDITY CORRELATION FUNCTIONS

In order to calculate correlation functions, the finite-size corrections to the ground-state energy and low-energy excitations are needed. There are now four energy branches rather than two as for the $S = 1/2$ case. The expression for the conformal towers is similar to the one presented in Sec. II, Eqs. (11) and (12), only that the indices l and q (representing the string length) now go from 0 to 3. The group velocities for the four branches of excitations are again given by Eq. (10).

The matrix of generalized dressed charges z_{lq} has now dimension 4×4. The situation is similar to that encountered for the degenerate supersymmetric t-J model[66] and the Coulomb drag between Luttinger liquids.[67] The dressed generalized charges are obtained as $z_{lq} = \xi_{lq}(B_q)$, where the ξ_{lq} are the solution of four sets of integral equations of the form of Eq. (22). The sets are labeled by the index $l = 0, \ldots, 3$ and yield $X^{(q)}(\xi) = \xi_{lq}(\xi)$ for the driving terms $D_q(\xi) = \delta_{l,q}$. There are then altogether 16 dressed charges to be calculated, which determine the interplay of the different Fermi points when a low-lying excitation is introduced. The dimension of the matrix is gradually reduced as the energy bands are depopulated, e.g., if there are only three bands occupied then the matrix is 3×3, etc.

There are four sets of four quantum numbers, one set for each band, describing the low-energy excitations of the Fermi liquid. As for the $S = 1/2$ case, each set l consists of a quantum number for the change in the number of particles in the band l, ΔN_l, a backward scattering quantum number D_l, and two quantum numbers for the particle-hole excitations at the Fermi points, $n_l^{\pm}$, for forward and backward movers, respectively. While $n_l^{\pm} = 0$ for the present purposes, ΔN_l and $2D_l$ take integer values. Hence, D_l can have integer or half-integer values. For elementary excitations from the ground state, the values of the D_l quantum numbers are constrained by the discrete Bethe *Ansatz* equations. A change in the population of band q, ΔN_q, changes the backscattering quantum numbers by

$$D_l = \tfrac{1}{2}[\min(l,q)+1]\Delta N_q \pmod 1 . \qquad (30)$$

Note that the D_l are only determined modulo 1, which gives rise to some degrees of freedom.

We now consider the operators associated with superfluidity in the Fermi gas. There are three classes of bound states that can lead to superfluidity, i.e., the creation of a four-particle bound state is characterized by $\Delta N_3 = 1$ and all other $\Delta N_l = 0$, the creation of a three-particle bound state is characterized by $\Delta N_2 = 1$ and all other $\Delta N_l = 0$, and a bound state of two particles (pair) by $\Delta N_1 = 1$ and all other $\Delta N_l = 0$. These are the quantum numbers classifying the operators. For each case, there may be more than just one set of quantum numbers D_l.

Let us first consider the pure phases, i.e., only one band is occupied. The case of pairs has been discussed in Sec. II D where we concluded that the quantum numbers are $\Delta N_1 = 1$ and $D_1 = 0$. In terms of atom creation operators this operator now reads $c^{\dagger}_{3/2+}c^{\dagger}_{1/2-}$, i.e., one forward mover coupled to a backward mover. The situation is similar if the four-particle bound states are considered. In this case the quantum numbers are $\Delta N_3 = 1$ and $D_3 = 0$, and one of the possible operators is $c^{\dagger}_{3/2+}c^{\dagger}_{1/2+}c^{\dagger}_{-1/2-}c^{\dagger}_{-3/2-}$, i.e., there are two forward and two backward movers involved. Less trivial is the case of three-particle bound states, because now the bound states carry momentum. With three particles two must be forward (backward) movers and the third particle is a backward (forward) mover. This leads to a momentum of πn_2 ($-\pi n_2$), and hence $D_2 = \pm 1/2$. These cases have been studied previously in Ref. 68 and the quantum numbers are listed in Table I.

TABLE I. Superfluidity operators and their quantum numbers. If more than one possible operator exists for a given set of quantum numbers, then only one of them is listed. ΔN_l is the change in the number of bound clusters of string-length l [$(l+1)$ particles] and D_l is the corresponding backward scattering (parity) quantum number. For the leading exponent, all particle-hole excitation quantum numbers, $n_l^{\pm}$, are zero. Here, λ is the distance between nodes in the corresponding term of the correlation function. The index in the last column is the label in Figs. 5, 6, 8, and 9.

Phase	Operator $\mathcal{O}^\dagger$	ΔN_0	ΔN_1	ΔN_2	ΔN_3	D_0	D_1	D_2	D_3	$1/\lambda$	Label
IV	$c^\dagger_{3/2,+}c^\dagger_{1/2,+}c^\dagger_{-1/2,-}c^\dagger_{-3/2,-}$	...	...	...	+1	...	...	...	0	0	
III	$c^\dagger_{3/2,+}c^\dagger_{1/2,+}c^\dagger_{-1/2,-}$	...	...	+1	...	...	...	$\pm\frac{1}{2}$	...	n_2	
II	$c^\dagger_{3/2,+}c^\dagger_{1/2,-}$	...	+1	...	...	...	0	...	...	0	
I + IV	$c^\dagger_{3/2,+}c^\dagger_{1/2,+}c^\dagger_{-1/2,-}c^\dagger_{-3/2,-}$	0	...	...	+1	$\pm\frac{1}{2}$	...	...	0	n_0	a,b,c
I + III	$c^\dagger_{3/2,+}c^\dagger_{1/2,+}c^\dagger_{-1/2,-}$	0	...	+1	...	$\pm\frac{1}{2}$	...	$\pm\frac{1}{2}$	...	n_0+n_2	
I + III	$c^\dagger_{3/2,+}c^\dagger_{1/2,-}c^\dagger_{-1/2,-}$	0	...	+1	...	$\pm\frac{1}{2}$	...	$\mp\frac{1}{2}$	...	$\lvert n_0-n_2\rvert$	
I + II	$c^\dagger_{3/2,+}c^\dagger_{1/2,+}$	0	+1	...	...	$\pm\frac{1}{2}$	±1	...	...	n_0+2n_1	α
I + II	$c^\dagger_{3/2,+}c^\dagger_{1/2,-}$	0	+1	...	...	$\pm\frac{1}{2}$	0	...	...	n_0	β
II + IV	$c^\dagger_{3/2,+}c^\dagger_{1/2,+}c^\dagger_{-1/2,-}c^\dagger_{-3/2,-}$	...	0	...	+1	...	±1	...	0	$2n_1$	
II + IV	$c^\dagger_{3/2,+}c^\dagger_{1/2,-}c^\dagger_{-1/2,+}c^\dagger_{-3/2,-}$	...	0	...	+1	...	0	...	0	0	
II + IV	$c^\dagger_{3/2,+}c^\dagger_{1/2,-}$	...	+1	...	0	...	0	...	0	0	
II + IV	$c^\dagger_{3/2,+}c^\dagger_{1/2,+}$	...	+1	...	0	...	±1	...	±1	$2(n_1+n_3)$	
III + IV	$c^\dagger_{3/2,+}c^\dagger_{1/2,+}c^\dagger_{-1/2,-}c^\dagger_{-3/2,-}$	...	...	0	+1	...	...	$\pm\frac{1}{2}$	0	n_2	
III + IV	$c^\dagger_{3/2,+}c^\dagger_{1/2,+}c^\dagger_{-1/2,-}$	...	...	+1	0	...	...	$\pm\frac{1}{2}$	$\pm\frac{1}{2}$	n_2+n_3	
II + III	$c^\dagger_{3/2,+}c^\dagger_{1/2,+}c^\dagger_{-1/2,-}$	...	0	+1	...	...	±1	$\pm\frac{1}{2}$	...	$2n_1+n_2$	
II + III	$c^\dagger_{3/2,+}c^\dagger_{1/2,-}c^\dagger_{-1/2,+}$	...	0	+1	...	...	0	$\pm\frac{1}{2}$	...	n_2	
II + III	$c^\dagger_{3/2,+}c^\dagger_{1/2,-}$	...	+1	0	...	...	0	0	...	0	
II + III	$c^\dagger_{3/2,+}c^\dagger_{1/2,+}$	...	+1	0	...	...	±1	±1	...	$2(n_1+n_2)$	
I + II + IV	$c^\dagger_{3/2,+}c^\dagger_{1/2,+}c^\dagger_{-1/2,-}c^\dagger_{-3/2,-}$	0	0	...	+1	$\pm\frac{1}{2}$	±1	...	0	n_0+2n_1	a
I + II + IV	$c^\dagger_{3/2,+}c^\dagger_{1/2,-}c^\dagger_{-1/2,+}c^\dagger_{-3/2,-}$	0	0	...	+1	$\pm\frac{1}{2}$	0	...	0	n_0	b,c
I + II + IV	$c^\dagger_{3/2,+}c^\dagger_{1/2,+}$	0	+1	...	0	$\pm\frac{1}{2}$	±1	...	±1	$n_0+2n_1+2n_3$	α
I + II + IV	$c^\dagger_{3/2,+}c^\dagger_{1/2,-}$	0	+1	...	0	$\pm\frac{1}{2}$	0	...	0	n_0	β
I + III + IV	$c^\dagger_{3/2,+}c^\dagger_{1/2,+}c^\dagger_{-1/2,-}c^\dagger_{-3/2,-}$	0	...	0	+1	$\pm\frac{1}{2}$	...	$\pm\frac{1}{2}$	0	n_0+n_2	
I + III + IV	$c^\dagger_{3/2,+}c^\dagger_{1/2,-}c^\dagger_{-1/2,-}c^\dagger_{-3/2,+}$	0	...	0	+1	$\pm\frac{1}{2}$	...	$\mp\frac{1}{2}$	0	$\lvert n_0-n_2\rvert$	
I + III + IV	$c^\dagger_{3/2,+}c^\dagger_{1/2,+}c^\dagger_{-1/2,-}$	0	...	+1	0	$\pm\frac{1}{2}$	...	$\pm\frac{1}{2}$	$\pm\frac{1}{2}$	$n_0+n_2+n_3$	
I + III + IV	$c^\dagger_{3/2,+}c^\dagger_{1/2,-}c^\dagger_{-1/2,-}$	0	...	+1	0	$\pm\frac{1}{2}$	...	$\mp\frac{1}{2}$	$\mp\frac{1}{2}$	$\lvert n_0-n_2-n_3\rvert$	
I + II + III	$c^\dagger_{3/2,+}c^\dagger_{1/2,+}c^\dagger_{-1/2,-}$	0	0	+1	...	$\pm\frac{1}{2}$	±1	$\pm\frac{1}{2}$	...	$n_0+2n_1+n_2$	a
I + II + III	$c^\dagger_{3/2,+}c^\dagger_{1/2,-}c^\dagger_{-1/2,+}$	0	0	+1	...	$\pm\frac{1}{2}$	0	$\pm\frac{1}{2}$	...	n_0+n_2	b
I + II + III	$c^\dagger_{3/2,+}c^\dagger_{1/2,-}c^\dagger_{-1/2,-}$	0	0	+1	...	$\pm\frac{1}{2}$	0	$\mp\frac{1}{2}$	...	$\lvert n_0-n_2\rvert$	c
I + II + III	$c^\dagger_{3/2,+}c^\dagger_{1/2,+}$	0	+1	0	...	$\pm\frac{1}{2}$	±1	±1	...	$n_0+2n_1+2n_2$	α
I + II + III	$c^\dagger_{3/2,+}c^\dagger_{1/2,-}$	0	+1	0	...	$\pm\frac{1}{2}$	0	0	...	n_0	β
II + III + IV	$c^\dagger_{3/2,+}c^\dagger_{1/2,+}c^\dagger_{-1/2,-}c^\dagger_{-3/2,-}$	...	0	0	+1	...	±1	$\pm\frac{1}{2}$	0	$2n_1+n_2$	
II + III + IV	$c^\dagger_{3/2,+}c^\dagger_{1/2,-}c^\dagger_{-1/2,+}c^\dagger_{-3/2,-}$	...	0	0	+1	...	0	$\pm\frac{1}{2}$	0	n_2	
II + III + IV	$c^\dagger_{3/2,+}c^\dagger_{1/2,+}c^\dagger_{-1/2,-}$	...	0	+1	0	...	±1	$\pm\frac{1}{2}$	$\pm\frac{1}{2}$	$2n_1+n_2+n_3$	
II + III + IV	$c^\dagger_{3/2,+}c^\dagger_{1/2,-}c^\dagger_{-1/2,+}$	...	0	+1	0	...	0	$\pm\frac{1}{2}$	$\pm\frac{1}{2}$	n_2+n_3	
II + III + IV	$c^\dagger_{3/2,+}c^\dagger_{1/2,+}$	...	+1	0	0	...	±1	±1	±1	$2(n_1+n_2+n_3)$	
II + III + IV	$c^\dagger_{3/2,+}c^\dagger_{1/2,-}$	...	+1	0	0	...	0	0	0	0	
I + II + III + IV	$c^\dagger_{3/2,+}c^\dagger_{1/2,+}c^\dagger_{-1/2,-}c^\dagger_{-3/2,-}$	0	0	0	+1	$\pm\frac{1}{2}$	±1	$\pm\frac{1}{2}$	0	$n_0+2n_1+n_2$	a
I + II + III + IV	$c^\dagger_{3/2,+}c^\dagger_{1/2,-}c^\dagger_{-1/2,+}c^\dagger_{-3/2,-}$	0	0	0	+1	$\pm\frac{1}{2}$	0	$\pm\frac{1}{2}$	0	n_0+n_2	b
I + II + III + IV	$c^\dagger_{3/2,+}c^\dagger_{1/2,-}c^\dagger_{-1/2,-}c^\dagger_{-3/2,+}$	0	0	0	+1	$\pm\frac{1}{2}$	0	$\mp\frac{1}{2}$	0	$\lvert n_0-n_2\rvert$	c
I + II + III + IV	$c^\dagger_{3/2,+}c^\dagger_{1/2,+}c^\dagger_{-1/2,-}$	0	0	+1	0	$\pm\frac{1}{2}$	±1	$\pm\frac{1}{2}$	$\pm\frac{1}{2}$	$n_0+2n_1+n_2+n_3$	a
I + II + III + IV	$c^\dagger_{3/2,+}c^\dagger_{1/2,-}c^\dagger_{-1/2,+}$	0	0	+1	0	$\pm\frac{1}{2}$	0	$\pm\frac{1}{2}$	$\pm\frac{1}{2}$	$n_0+n_2+n_3$	b
I + II + III + IV	$c^\dagger_{3/2,+}c^\dagger_{1/2,-}c^\dagger_{-1/2,-}$	0	0	+1	0	$\pm\frac{1}{2}$	0	$\mp\frac{1}{2}$	$\mp\frac{1}{2}$	$\lvert n_0-n_2-n_3\rvert$	c
I + II + III + IV	$c^\dagger_{3/2,+}c^\dagger_{1/2,+}$	0	+1	0	0	$\pm\frac{1}{2}$	±1	±1	±1	$n_0+2n_1+2n_2+2n_3$	α
I + II + III + IV	$c^\dagger_{3/2,+}c^\dagger_{1/2,-}$	0	+1	0	0	$\pm\frac{1}{2}$	0	0	0	n_0	β

The quantum numbers of the mixed phases are harder to figure out. The phase I + II has been studied in Sec. II and the relevant operators have quantum numbers $\Delta N_1 = 1$ and $D_0 = \pm 1/2$, while D_1 is an integer, 0 or 1. Similarly for I + IV, $\Delta N_3 = 1$, $\Delta N_0 = 0$, $D_0 = \pm 1/2$, and D_3 is an integer, which we choose 0 (two forward and two backward movers). Finally, for I + III, we have $\Delta N_2 = 1$, $D_0 = \pm 1/2$, and D_2 either $\pm 1/2$ or $\mp 1/2$. Hence, in this case, there are two sets of quantum numbers and, consequently, two operators for the same phase. The occupations of the bands are $n_{3/2} = n_0 + n_2$ and $n_{\pm 1/2} = n_2$, while $n_{-3/2} = 0$. In terms of atom creation operators, these operators are $c^\dagger_{3/2,\pm} c^\dagger_{1/2,\pm} c^\dagger_{-1/2,\mp}$ and $c^\dagger_{3/2,\pm} c^\dagger_{1/2,\mp} c^\dagger_{-1/2,\mp}$, where again the $+/-$ signs refer to forward/backward movers. Hence, there are two competing correlation functions and the one with smaller critical exponent is expected to be the dominant one.

For the mixed phase II + IV, the population of the levels are $n_{3/2} = n_{1/2} = n_1 + n_3$ and $n_{-1/2} = n_{-3/2} = n_3$. There are four operators for superfluidity, two corresponding to $\Delta N_3 = 1$, $c^\dagger_{3/2,\pm} c^\dagger_{1/2,\pm} c^\dagger_{-1/2,\mp} c^\dagger_{-3/2,\mp}$ and $c^\dagger_{3/2,\pm} c^\dagger_{1/2,\mp} c^\dagger_{-1/2,\pm} c^\dagger_{-3/2,\mp}$, and two to $\Delta N_1 = 1$, $c^\dagger_{3/2,\pm} c^\dagger_{1/2,\mp}$ and $c^\dagger_{3/2,\pm} c^\dagger_{1/2,\pm}$. The backscattering quantum numbers D_q can now be determined. For the first $\Delta N_3 = 1$ operator only $D_1 = \pm 1$ is different from zero, for the second operator, all D_q vanish, while for the first $\Delta N_1 = 1$ operator all $D_q = 0$ and for the second, $D_1 = D_3 = \pm 1$.

For the mixed phase III + IV, $n_{3/2} = n_{1/2} = n_{-1/2} = n_2 + n_3$ and $n_{-3/2} = n_3$, there are three operators with $\Delta N_3 = 1$, $c^\dagger_{3/2,\pm} c^\dagger_{1/2,\mp} c^\dagger_{-1/2,\pm} c^\dagger_{-3/2,\mp}$, $c^\dagger_{3/2,\pm} c^\dagger_{1/2,\pm} c^\dagger_{-1/2,\mp} c^\dagger_{-3/2,\mp}$, and $c^\dagger_{3/2,\pm} c^\dagger_{1/2,\mp} c^\dagger_{-1/2,\mp} c^\dagger_{-3/2,\pm}$, yielding $D_2 = \pm 1/2$ while all other $D_q = 0$. For $\Delta N_2 = 1$, there are three operators, $c^\dagger_{3/2,\pm} c^\dagger_{1/2,\mp} c^\dagger_{-1/2,\pm}$, $c^\dagger_{3/2,\pm} c^\dagger_{1/2,\pm} c^\dagger_{-1/2,\mp}$, and $c^\dagger_{3/2,\pm} c^\dagger_{1/2,\mp} c^\dagger_{-1/2,\mp}$, yielding $D_2 = D_3 = \pm 1/2$.

In the phase II + III, $n_{3/2} = n_{1/2} = n_1 + n_2$, $n_{-1/2} = n_2$, and $n_{-3/2} = 0$, there are again two pair correlation functions, $c^\dagger_{3/2,\pm} c^\dagger_{1/2,\mp}$ and $c^\dagger_{3/2,\pm} c^\dagger_{1/2,\pm}$. The corresponding quantum numbers are $\Delta N_1 = 1$, and $D_2 = D_1 = 0$ and $D_2 = D_1 = \pm 1$, respectively. There are also three

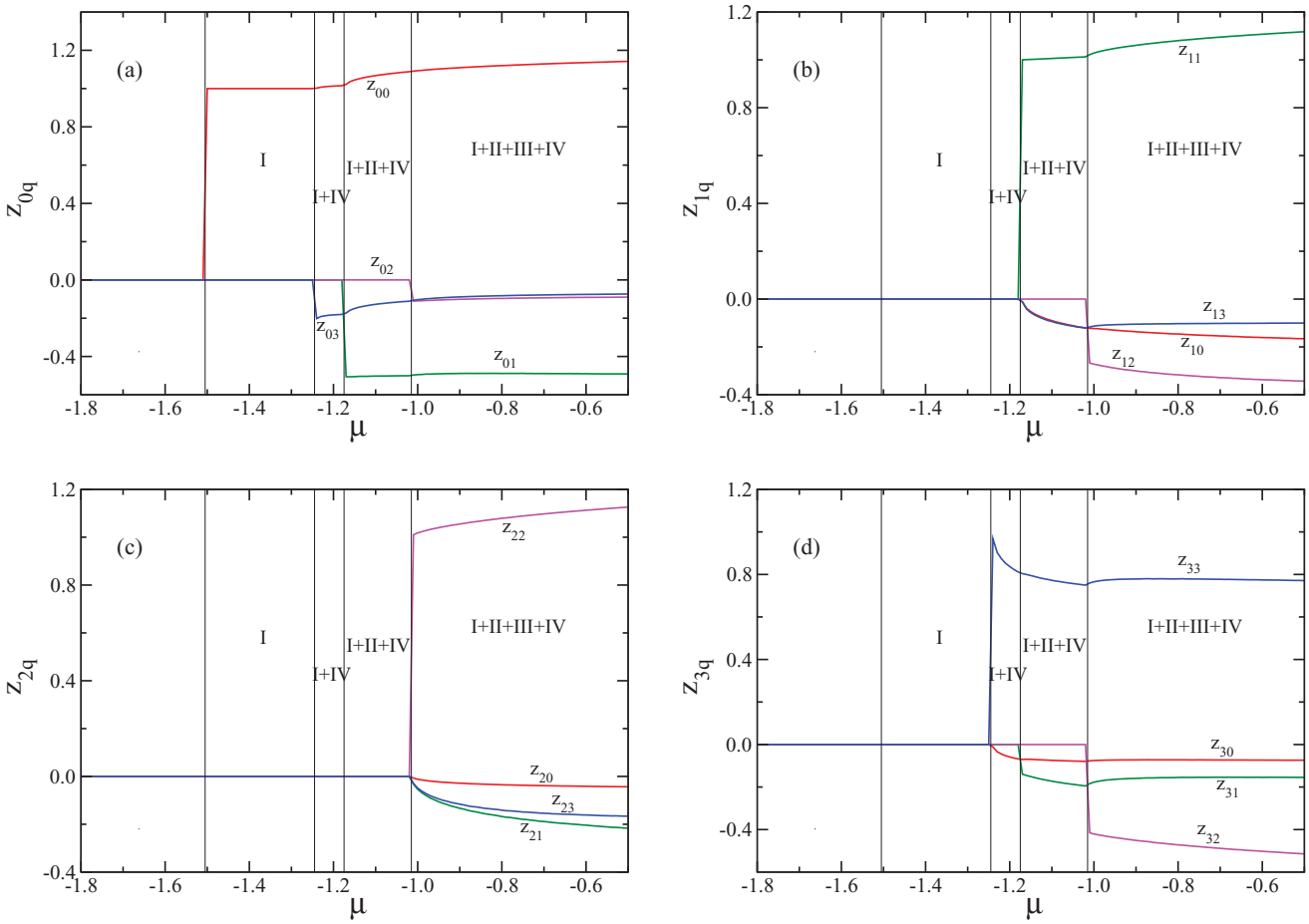

FIG. 4. (Color online) Dressed generalized charges for a homogeneous fermion gas of spin $S = 3/2$ with $|c| = 1$ and $H = 1.0$ as a function of μ. $H = 1.0$ corresponds to one of the dashed vertical lines in Fig. 2. The z_{lq} determine the interplay between the different Fermi points in the system. The thin vertical lines refer to the crossing between different phases. (a) corresponds to $l = 0$, i.e. z_{0q}, panel (b) to $l = 1$ (z_{1q}), panel (c) to $l = 2$ (z_{2q}) and panel (d) to $l = 3$ (z_{3q}). All dressed generalized charges are different from zero for the mixed phase I + II + III + IV. As the individual phases disappear with decreasing μ the effective dimension of $\hat{z}$ is reduced. The curves for $q = 0$ are in red, the ones for $q = 1$ are green, magenta the ones for $q = 2$ and blue if $q = 3$. Note that many of the charges vary discontinuously at the transitions.

$\Delta N_2 = 1$ operators, $c^\dagger_{3/2,\pm}c^\dagger_{1/2,\pm}c^\dagger_{-1/2,\mp}$, $c^\dagger_{3/2,\pm}c^\dagger_{1/2,\mp}c^\dagger_{-1/2,\pm}$ and $c^\dagger_{3/2,\pm}c^\dagger_{1/2,\mp}c^\dagger_{-1/2,\mp}$, yielding $D_1 = \pm 1$ and $D_2 = \pm 1/2$ for the first operator and $D_1 = 0$ and $D_2 = \pm 1/2$ for the remaining two operators. It is more tedious to obtain the quantum numbers for mixed phases with three or four bands. The most relevant sets of possible quantum numbers contributing to correlation functions for superfluidity are displayed in Table I.

The superfluidity correlation functions can now be calculated. The procedure is analogous to that for Cooper pairs in Sec. II D. For each operator $\mathcal{O}^\dagger$ in Table I the correlation function is similar to expression (14), only that the product in the denominator is from $l = 0, \ldots, 4$ and $D_0 p_0 + D_1 p_1$ in the exponential is to be replaced by $\sum_{l=0}^4 D_l p_l = \sum_{l=0}^4 2\pi D_l n_l$. The conformal dimensions are defined as

$$2\Delta_l^\pm = 2n_l^\pm + \left[\sum_{q=0}^{3} z_{ql} D_q \pm \frac{1}{2}\sum_{q=0}^{3}(\hat{z}^{-1})_{lq}\Delta N_q\right]^2 . \quad (31)$$

The leading terms of the equal time correlation function for the $\mathcal{O}^\dagger$ operators are then of the form (all $n_q^\pm = 0$)

$$\langle \mathcal{O}^\dagger(x,0)\mathcal{O}(0,0)\rangle = A x^{-\theta}\cos(\pi x/\lambda) \quad (32)$$

for the phase under consideration. The amplitude A cannot be determined from conformal field theory. The exponent θ is given by

$$\theta = 2\sum_{q=0}^{3}(\Delta_q^+ + \Delta_q^-), \quad n_q^\pm = 0 \quad (33)$$

and the distance between nodes λ is given by $1/|2\sum_{q=0}^4 D_q n_q|$. The expressions for $1/\lambda$ are shown in Table I in the column previous to the last one. Note that for fixed μ/c^2 and H/c^2, the dressed generalized charges and hence the exponents θ are independent of the coupling strength $|c|$.

V. RESULTS

In this section, we discuss the matrix of dressed generalized charges, critical exponents, and the periods of oscillation of the correlation functions along the vertical (dashed) lines in Fig. 2, i.e., $H = 1.0$ and $H = 2.0$. These two examples correspond to two very different situations.

A. The $H = 1.0$ line

The components of the matrix of dressed generalized charges for a homogeneous Fermi gas for $|c| = 1$, $S = 3/2$ and $H = 1.0$ as a function of μ are displayed in Fig. 4. The z_{lq} determine the interplay between the different Fermi points in the system. The thin vertical lines refer to the transitions between the different phases. The four panels show (a) z_{0q}, (b) z_{1q}, (c) z_{2q}, and (d) z_{3q}, with $q = 0, \ldots, 3$. With decreasing μ the dressed energy bands gradually are emptied and the effective dimension of $\hat{z}$ is reduced as the individual phases disappear. All dressed generalized charges are different from zero for the phase mixed I + II + III + IV. In general, the z_{lq} for $l \neq q$ are always negative, while diagonal elements are positive. Note that many of the charges vary discontinuously at the transitions.

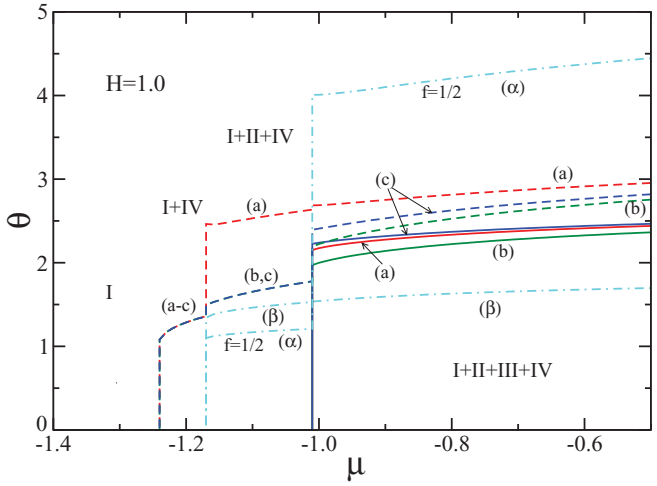

FIG. 5. (Color online) Critical exponents for the correlation functions for $S = 3/2$ with $H = 1.0$ and $|c| = 1$ as a function of μ. $H = 1.0$ corresponds to one of the dashed vertical lines in Fig. 2. The exponents are all discontinuous at the transitions. The dashed curves correspond to the four-particle bound state correlation functions, the solid curves to the three-particle bound state responses and the dash-dotted curves to the pairs (cyan). According to Table I there are three three- and four-particle correlators in the mixed phase I + II + III + IV; they are denoted with (a) (red), (b) (green), and (c) (blue). There are two four-particle correlation functions in the phase I + II + IV. There are also two correlation functions for pairs denoted by (α) and (β), respectively. Note that curve (α) has been rescaled by a factor of $f = 1/2$.

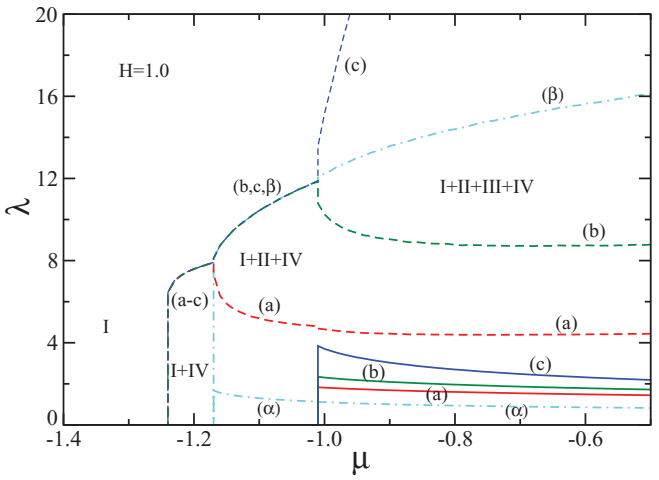

FIG. 6. (Color online) Distance between nodes of the correlation functions for $S = 3/2$ with $H = 1.0$ and $|c| = 1$ as a function of μ. $H = 1.0$ corresponds to one of the dashed vertical lines in Fig. 2. Some of the periods of spatial oscillation are discontinuous at the transitions between the phases. The dashed curves correspond to the four-particle bound-state correlation functions, the solid curves to the three-particle bound state responses and the dash-dotted curves to the pairs (cyan). According to Table I, there are three three- and four-particle correlators in the mixed phase I + II + III + IV; they are denoted with (a) (red), (b) (green), and (c) (blue). There are two four-particle correlation functions in the phase I + II + IV. There are also two correlation functions for pairs denoted by α and β, respectively.

Figure 5 presents the critical exponents for the same parameters as Fig. 4. The exponents of the pair correlation functions (pairing of particles with $S_z = 3/2$ and $1/2$) are shown as the dashed dotted (cyan) curves and denoted with α and β, respectively. Note that the curve α has been reduced by a factor $1/2$. The operator corresponding to curve α carries a large momentum, $\pi(n_0 + 2n_1 + 2n_2 + 2n_3)$, while the momentum of the operator for β is just πn_0. The exponent of β is the smallest of all exponents and, hence, this correlation function has the longest range.

There are three three-particle and three four-particle correlation functions in the I + II + III + IV phase. Only the four-particle responses survive into the I + II + IV and I + IV phases. The green curves [denoted with (b)] have the smallest exponent and, hence, these correlation functions are the ones with longest range within the ΔN_2 and ΔN_3 categories, since they have the slowest decay with distance. The wave numbers of the oscillation are $\pi(n_0 + n_2 + n_3)$ and $\pi(n_0 + n_2)$, respectively.

Figure 6 displays the corresponding distance between nodes, λ, that appears in the oscillating factor. The λ for the dominant response functions for three- and four-particle bound states are the green curves denoted with (b). The corresponding one for the pair correlation function (β) is shown as the (cyan) dash-dotted curve.

As discussed in Sec. II, in the presence of an array of tubes, there is the possibility of Josephson tunneling of individual particles, pairs and three- and four-particle bound states, which eventually will give rise to superfluid long-range order.[1,21,47] The order is quasi-one-dimensional, since the particles predominantly move along the tubes, i.e., the Fermi surfaces remain being one-dimensional, but there is coherence between the different tubes. The Luttinger liquid properties remain then valid in the disordered phase and the one-dimensional correlations functions determine the three-dimensional order. There is a fundamental difference with the ordinary BCS theory because the bound states are preformed and already exist in the normal phase. The binding energy of Cooper pairs due to long-range order is the primary energy gain for superconductivity in the BCS theory, but that is not the case for the present quasiparticles, since the bound states are preformed.

It is a difficult task to figure out which operator is the one leading to finite T superfluidity from the normal phase. There

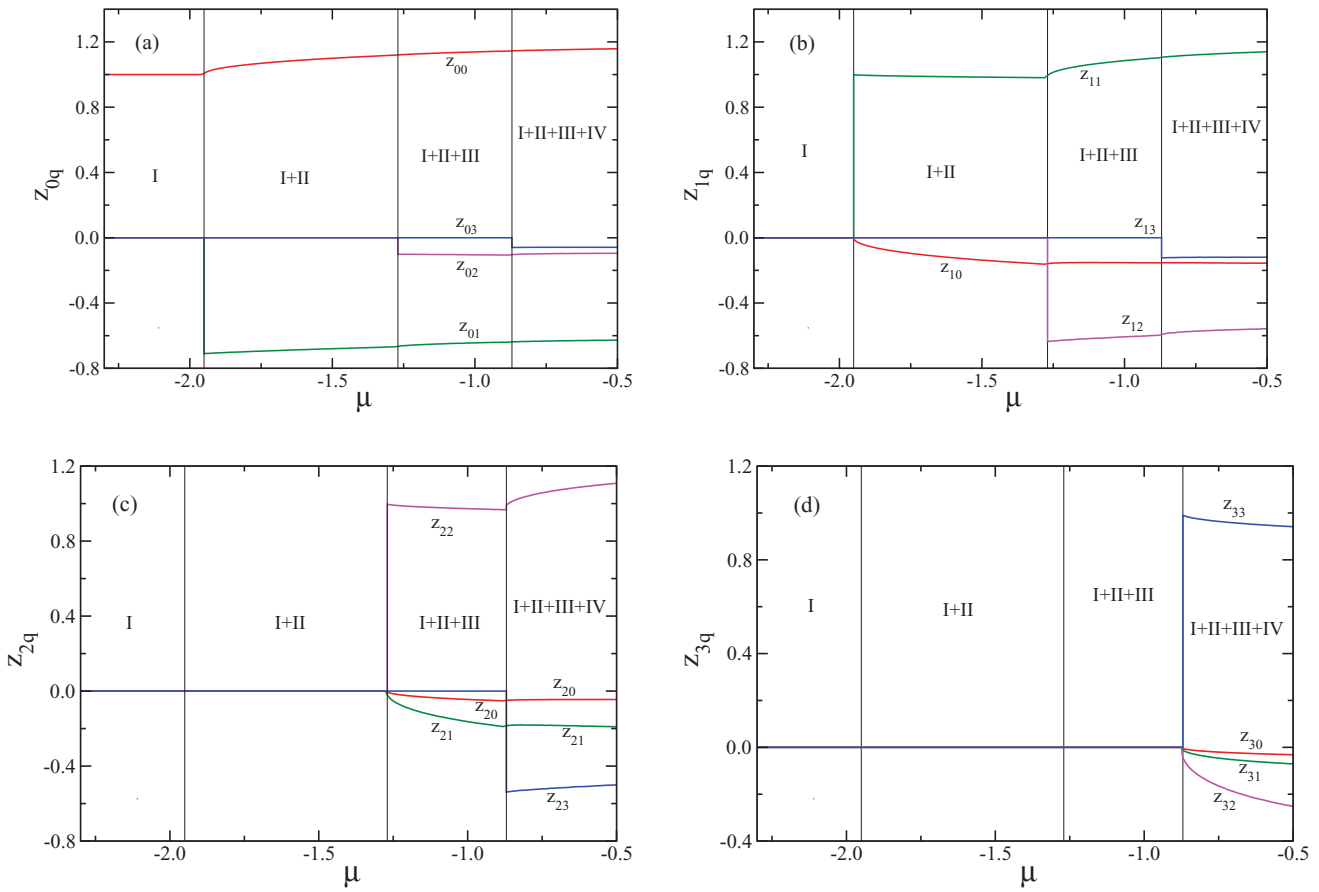

FIG. 7. (Color online) Dressed generalized charges for a homogeneous fermion gas of spin $S = 3/2$ with $|c| = 1$ and $H = 2.0$ as a function of μ. $H = 2.0$ corresponds to one of the dashed vertical lines in Fig. 2. The z_{lq} determine the interplay between the different Fermi points in the system. The thin vertical lines refer to the crossing between different phases. (a) corresponds to $l = 0$, i.e., z_{0q}, panel (b) to $l = 1$ (z_{1q}), panel (c) to $l = 2$ (z_{2q}) and panel (d) to $l = 3$ (z_{3q}). All dressed generalized charges are different from zero for the mixed phase I + II + III + IV. As the individual phases disappear with decreasing μ the effective dimension of $\hat{z}$ is reduced. The curves for $q = 0$ are in red, the ones for $q = 1$ are green, magenta the ones for $q = 2$ and blue if $q = 3$. Note that some of the charges vary discontinuously at the transitions.

are three possible criteria (i) the correlation function with the smallest exponent θ is the one with the longest range, (ii) a large λ favors order because nodes in the order parameter are generally energetically unfavorable, and (iii) the bound states should have a small momentum, since a large momentum of the bound states is unfavorable to a condensate. The critical scaling dimension in one dimension is 2, so that only operators with a θ less than 2 are favorable to order. The conditions (ii) and (iii) are related with each other. The argument that it is unfavorable to create large momentum carrying bound states can be ruled out because their binding energy is already build into the Bethe *Ansatz* solution of the model. The long-range order is expected to have similar properties as the ones predicted by Fulde, Ferrell, Ovchinnikov, and Larkin,[46] i.e., the order parameter is modulated. The period of the sinusoidal modulation is given by the momentum differences of the Fermi points involved and, hence, the same as the one given by λ in the present calculation.

The dominant correlation function is the one expected to give rise to the strongest long-range order parameter. An additional variable entering the problem is, which bound states can tunnel most efficiently between tubes. We will assume that the tunneling amplitude is about the same for all the bound states. From Fig. 5, we see that the pairing operator [(β), dash-dotted, cyan] has the smallest exponent θ and a relatively large distance between nodes, λ. Pairing is also the only operator satisfying $\theta < 2$ throughout all the phases. Hence pairing appears to be the most favorable for the first superfluid ordered phase when coming from the normal phase. Other superfluid phases are expected to emerge at lower temperatures.

B. The $H = 2.0$ line

The sequence of phases along the $H = 2.0$ line is different from that along the $H = 1.0$ line. For $H = 2.0$ at large μ, all four bands are partially occupied (I + II + III + IV mixed phase) and as μ decreases first the IV phase disappears, then the III phase and finally the pairs, leaving only spin-polarized unpaired particles. The components of the matrix of dressed generalized charges for $|c| = 1$ and $S = 3/2$ are presented in Fig. 7 as a function of μ. The thin vertical lines refer to the transitions between the different phases. Again, all diagonal z_{lq} are positive and all off-diagonal elements are negative. Again, all dressed generalized charges are different from zero for the phase mixed I + II + III + IV. As the phases drop out as a function of μ the dimension of the matrix is reduced accordingly. Some of the dressed generalized charges vary discontinuously at the phase transitions. The discussion on the FFLO phase in Sec. V A remains valid here. The spatial oscillation of the order parameter is given by the respective λ.

The critical exponents for the same parameters as in Fig. 7 are displayed in Fig. 8. As for the $H = 1.0$ case, there are two two-particle, three three-particle, and three four-particle correlation functions in the I + II + III + IV phase. With decreasing μ, first the four-particle correlators disappear, then the three-particle response functions, and finally, the Cooper-pair functions. The dominant four-particle operators correspond to curves (b) and (c) (dashed, green and blue, respectively), which carry a smaller momentum as compared to (a). On the other hand, curves (a) and (b) (solid, red and green, respectively) correspond to the dominant exponents for

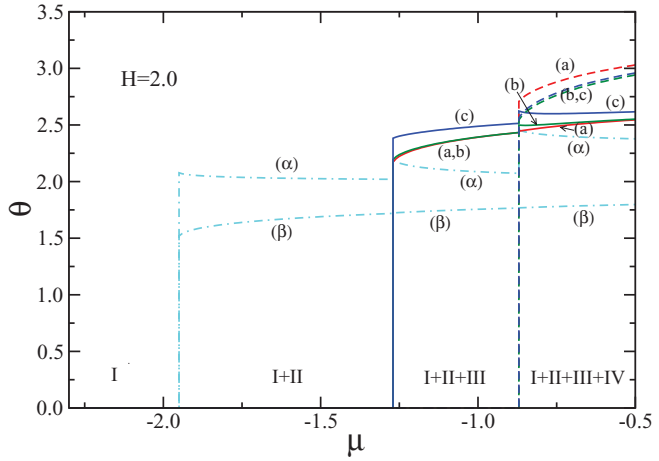

FIG. 8. (Color online) Critical exponents for the correlation functions for $S = 3/2$ with $H = 2.0$ and $|c| = 1$ as a function of μ. $H = 2.0$ corresponds to one of the dashed vertical lines in Fig. 2. The exponents are all discontinuous at the transitions. The dashed curves correspond to the four-particle bound state correlation functions, the solid curves to the three-particle bound state responses and the dash-dotted curves to the pairs (cyan). According to Table I, there are three three- and four-particle correlators in the mixed phase I + II + III + IV; they are denoted with (a) (red), (b) (green), and (c) (blue). There are three $\Delta N_2 = 1$ correlation functions in the phase I + II + III. There are also two correlation functions for pairs denoted by (α) and (β), respectively.

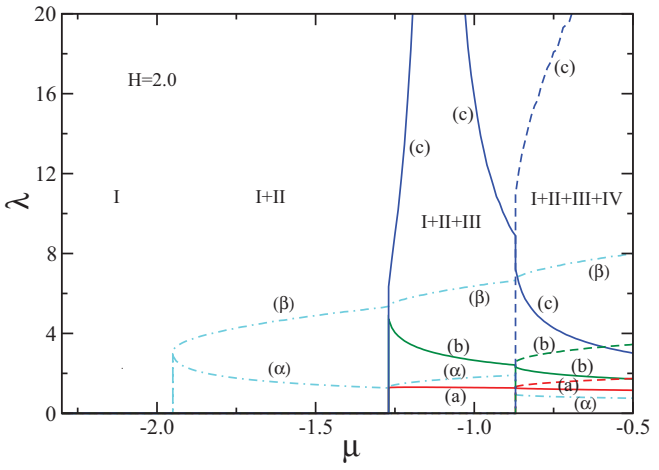

FIG. 9. (Color online) Distance between nodes of the correlation functions for $S = 3/2$ with $H = 2.0$ and $|c| = 1$ as a function of μ. $H = 2.0$ corresponds to one of the dashed vertical lines in Fig. 2. Some of the periods of spatial oscillation are discontinuous at the transitions between the phases. The dashed curves correspond to the four-particle bound state correlation functions, the solid curve to the three-particle bound state responses and the dash-dotted curves to the pairs (cyan). According to Table I, there are three three- and four-particle correlators in the mixed phase I + II + III + IV; they are denoted with (a) (red), (b) (green), and (c) (blue). There are three three-particle correlation functions in the phase I + II + III. There are also two correlation functions for pairs denoted by α and β, respectively.

the three-particle bound states. There are two exponents for the pair correlation functions denoted with α and β (cyan dashed dotted curves). Among the pair correlation functions, the β curve corresponds to the operator carrying the smaller momentum, πn_0, and has the lowest critical exponent. This response function has the most extended correlations in all phases and again is the only one with a θ below the critical scaling dimension of 2.

Figure 9 shows the corresponding distance between nodes, λ, arising from the sinusoidal factor. For the four-particle bound states, this distance is very long for curve (c) and shorter for curve (b). This makes (c) the more likely candidate for an instability among the four-particle bound states. For the same reason, (b) is the most likely candidate among the three-particle bound states. For pairs, the candidate is curve β, shown as the dashed-dotted cyan curve in Fig. 9. Again, the pairs β are the most likely candidate for order from the normal phase. Other phases are expected to emerge at lower temperatures.

VI. CONCLUSIONS

We studied an ultracold gas of fermionic atoms with $S = 3/2$ interacting via an attractive contact potential by solving the corresponding Bethe *Ansatz* equations and obtained the phase diagram in a magnetic field (μ versus H) within the grand-canonical ensemble. Four elementary states can occur: (i) polarized unbound atoms with spin-component $S_z = 3/2$, (ii) bound pairs of atoms with spin-components $S_z = 3/2$ and $1/2$, (iii) bound states of three particles with spin-components $S_z = 3/2$, $1/2$, and $-1/2$, and (iv) bound states of four particles, one with each spin-component. Mixed phases of different classes of bound states dominate the phase diagram. For a given chemical potential, the phases are homogeneous and display no long-range order. The transitions between phases are crossovers of the Prokovskii-Talapov type. The phase diagram for larger spin values has been obtained the same way,[39] but the calculations and the results are considerably more involved and complicated. Possible applications are to ultracold Fermi gases of ^{40}K (spin 9/2), ^{43}Ca (spin 7/2), ^{87}Sr (spin 9/2), ^{173}Yb (spin 5/2), ^{9}Be (spin 3/2), ^{135}Ba (spin 3/2), ^{137}Ba (spin 3/2), and ^{53}Cr (spin 3/2) atoms.

We investigated the possibility of finding inhomogeneous phases in the gas of two types: (a) we considered the scenario of phase separation along the tube and (b) modulations of the order parameters of the FFLO type. In case (a), the confining harmonic potential varies with the position along the tube. Within the local density approximation, which absorbs this variation into the chemical potential, μ is a function of x, and hence different phases are represented along the trap giving rise to phase separation.[1–3]

In case (b), inhomogeneities like modulations of the order parameter of the FFLO type, may arise in an array of tubes from Josephson tunneling between tubes and interactions between particles in different tubes.[21,47] This gives rise to a dimensional crossover from one-dimension to a higher dimension and opens the possibility for superfluid long-range order. The response functions in the disordered phase still have the Luttinger properties of the one-dimensional gas. These correlation functions determine the instability toward superfluidity from the normal phase. There are three possible criteria for the dominating order: (i) the correlation function with the smallest exponent θ is the one with the longest range and hence favorable if $\theta < 2$, i.e., less than the critical scaling dimension, (ii) a large λ favors order because nodes in the order parameter are further apart and hence energetically less unfavorable, and (iii) the bound states should carry a small momentum, since a large momentum of the bound states is unfavorable to a condensate.

There are three possible order parameters for superfluidity, namely, pairs of the Cooper type, three-particle bound states and four-particle bound states. The corresponding correlation functions have been calculated using conformal field theory. The calculation reveals that bound pairs are the bound states most likely to yield long-range order. The equal time response functions consist of the product of a power-law dependence of distance and a sinusoidal dependence of x. The oscillating factor is determined by the population imbalance of the different bands and is the same to be expected in the space modulation of the FFLO order parameters. This calculation is the extension of FFLO to spins larger than 1/2.[21] Note that the two main conditions for realization of the FFLO phase are satisfied in cold atom tubes: (1) the system is very pure (no impurities) and (2) it has a low effective dimension (extreme anisotropy).

ACKNOWLEDGMENTS

P.S. is supported by the US Department of Energy under Grant DE-FG02-98ER45707. A.A.Z. acknowledges the support from the Institute of Chemistry of V. N. Karazin Kharkov National University.

[1] Y. A. Liao, A. S. C. Rittner, T. Paprotta, W. H. Li, G. B. Partridge, R. G. Hulet, S. K. Baur, and E. J. Mueller, Nature (London) **467**, 567 (2010).

[2] G. Orso, Phys. Rev. Lett. **98**, 070402 (2007).

[3] H. Hu, X.-J. Liu, and P. D. Drummond, Phys. Rev. Lett. **98**, 070403 (2007).

[4] M. Olshanii, Phys. Rev. Lett. **81**, 938 (1998).

[5] T. Bergeman, M. G. Moore, and M. Olshanii, Phys. Rev. Lett. **91**, 163201 (2003).

[6] M. W. Zwierlein, A. Schirotzek, C. H. Schunck, and W. Ketterle, Science **311**, 492 (2006); Nature (London) **442**, 54 (2006).

[7] Y. Shin, M. W. Zwierlein, C. H. Schunck, A. Schirotzek, and W. Ketterle, Phys. Rev. Lett. **97**, 030401 (2006); C. H. Schunck, Y. Shin, A. Schirotzek, M. W. Zwierlein, and W. Ketterle, Science **316**, 867 (2007).

[8] G. B. Partridge, W. H. Li, R. I. Kamar, Y. A. Liao, and R. G. Hulet, Science **311**, 503 (2006); G. B. Partridge, W. H. Li, Y. A. Liao, R. G. Hulet, M. Haque, and H. T. C. Stoof, Phys. Rev. Lett. **97**, 190407 (2006).

[9] J. S. Krauser, J. Heinze, N. Fläschner, S. Götze, C. Becker, and K. Sengstock, e-print arXiv:1203.0948.

[10] M. Gaudin, Phys. Lett. A **24**, 55 (1967).

[11]C. N. Yang, Phys. Rev. Lett. **19**, 1312 (1967).
[12]M. Takahashi, Prog. Theor. Phys. **46**, 1388 (1971).
[13]C. K. Lai, Phys. Rev. Lett. **26**, 1472 (1971); Phys. Rev. A **8**, 2567 (1973).
[14]T. B. Bahder and F. Woynarovich, Phys. Rev. B **33**, 2114 (1986).
[15]Kong-Ju-Bock Lee and P. Schlottmann, Phys. Rev. B **40**, 9104 (1989).
[16]T. Mizushima, K. Machida, and M. Ichioka, Phys. Rev. Lett. **94**, 060404 (2005).
[17]A. E. Feiguin and F. Heidrich-Meisner, Phys. Rev. B **76**, 220508 (2007).
[18]M. Casula, D. M. Ceperley, and E. J. Mueller, Phys. Rev. A **78**, 033607 (2008).
[19]X. W. Guan, M. T. Batchelor, C. Lee, and M. Bortz, Phys. Rev. B **76**, 085120 (2007).
[20]P. Kakashvili and C. J. Bolech, Phys. Rev. A **79**, 041603(R) (2009).
[21]K. Yang, Phys. Rev. B **63**, 140511(R) (2001).
[22]J. N. Fuchs, A. Recati, and W. Zwerger, Phys. Rev. Lett. **93**, 090408 (2004).
[23]I. V. Tokatly, Phys. Rev. Lett. **93**, 090405 (2004).
[24]A. Lüscher, R. M. Noack, and A. M. Läuchli, Phys. Rev. A **78**, 013637 (2008).
[25]E. Zhao and W. V. Liu, Phys. Rev. A **78**, 063605 (2008).
[26]E. Zhao, X.-W. Guan, W. V. Liu, M. T. Batchelor, and M. Oshikawa, Phys. Rev. Lett. **103**, 140404 (2009).
[27]E. Burovski, G. Orso, and T. Jolicoeur, Phys. Rev. Lett. **103**, 215301 (2009).
[28]J. Y. Lee and X.-W. Guan, Nucl. Phys. B **853** [FS], 125 (2011).
[29]B. Sutherland, Phys. Rev. Lett. **20**, 98 (1968).
[30]M. Takahashi, Prog. Theor. Phys. **44**, 899 (1970).
[31]C. H. Gu and C. N. Yang, Commun. Math. Phys. **122**, 105 (1989).
[32]P. Schlottmann, J. Phys.: Condens. Matter **5**, 5869 (1993).
[33]P. Schlottmann, J. Phys.: Condens. Matter **6**, 1359 (1994).
[34]P. Schlottmann, Int. J. Mod. Phys. B **11**, 355 (1997).
[35]X. W. Guan, M. T. Batchelor, C. Lee, and H.-Q. Zhou, Phys. Rev. Lett. **100**, 200401 (2008).
[36]X. W. Guan, M. T. Batchelor, C. Lee, and J. Y. Lee, Europhys. Lett. **86**, 50003 (2009).
[37]X. W. Guan, J. Y. Lee, M. T. Batchelor, X. G. Yin, and S. Chen, Phys. Rev. A **82**, 021606(R) (2010).
[38]P. He, X.-G. Yin, X. W. Guan, M. T. Batchelor, and Y. Wang, Phys. Rev. A **82**, 053633 (2010).
[39]P. Schlottmann and A. A. Zvyagin, Phys. Rev. B **85**, 024535 (2012).
[40]C. Wu, J.-P. Hu, and S.-C. Zhang, Phys. Rev. Lett. **91**, 186402 (2003).
[41]C. Wu and S.-C. Zhang, Phys. Rev. B **71**, 155115 (2005).
[42]C. Wu, Phys. Rev. Lett. **95**, 266404 (2005).
[43]J. Cao, Y. Jiang, and Y. Wang, Europhys. Lett. **87**, 30005 (2007).
[44]Y. Jiang, J. Cao, and Y. Wang, Europhys. Lett. **79**, 10006 (2009).
[45]Y. Jiang, J. Cao, and Y. Wang, J. Phys. A: Math. Theor. **44**, 345001 (2011).
[46]P. Fulde and A. Ferrell, Phys. Rev. A **135**, 550 (1964); A. Larkin and Y. N. Ovchinnikov, Zh. Eksp. Teor. Fiz. **47**, 1136 (1964) [Sov. Phys. JETP **20**, 762 (1965)].
[47]M. M. Parish, S. K. Baur, E. J. Mueller, and D. A. Huse, Phys. Rev. Lett. **99**, 250403 (2007).
[48]H. Radovan, N. A. Fortune, T. P. Murphy, S. T. Hannahs, E. C. Palm, S. W. Tozer, and D. Hall, Nature (London) **425**, 51 (2003).
[49]A. D. Bianchi, R. Movshovich, C. Capan, P. G. Pagliuso, and J. L. Sarrao, Phys. Rev. Lett. **91**, 187004 (2003).
[50]M. Kenzelmann, S. Gerber, N. Egetenmeyer, J. L. Gavilano, T. Strässle, A. D. Bianchi, E. Ressouche, R. Movshovich, E. D. Bauer, J. L. Sarrao, and J. D. Thompson, Phys. Rev. Lett. **104**, 127001 (2010).
[51]S. Uji, T. Terashima, M. Nishimura, Y. Takahide, T. Konoike, K. Enomoto, H. Cui, H. Kobayashi, A. Kobayashi, H. Tanaka, M. Tokumoto, E. S. Choi, T. Tokumoto, D. Graf, and J. S. Brooks, Phys. Rev. Lett. **97**, 157001 (2006).
[52]S. Yonezawa, S. Kusaba, Y. Maeno, P. Auban-Senzier, C. Pasquier, K. Bechgaard, and D. Jérome, Phys. Rev. Lett. **100**, 117002 (2008).
[53]F. Woynarovich, J. Phys. A **22**, 4243 (1989).
[54]A. G. Izergin, V. E. Korepin, and N. Yu. Reshetikhin, J. Phys. A **22**, 2615 (1989).
[55]H. Frahm and V. E. Korepin, Phys. Rev. B **42**, 10553 (1990).
[56]M. Pustilnik, M. Khodas, A. Kamenev, and L. I. Glazman, Phys. Rev. Lett. **96**, 196405 (2006).
[57]R. G. Pereira, J. Sirker, J.-S. Caux, R. Hagemans, J. M. Maillet, S. R. White, and I. Affleck, Phys. Rev. Lett. **96**, 257202 (2006).
[58]M. B. Zvonarev, V. V. Cheianov, and T. Giamarchi, Phys. Rev. Lett. **99**, 240404 (2007).
[59]F. H. L. Essler, Phys. Rev. B **81**, 205120 (2010).
[60]P. Schlottmann, J. Stat. Mech. (2006) P12003.
[61]P. Schlottmann, Z. Phys. **54**, 207 (1984).
[62]A. M. Tsvelick, J. Phys. C **17**, 2299 (1984).
[63]N. Kawakami, S. Tokuono, and A. Okiji, J. Phys. Soc. Jpn. **53**, 51 (1984).
[64]P. Schlottmann, Phys. Rep. **181**, 1 (1989).
[65]P. Schlottmann, Phys. Rev. B **36**, 5177 (1987).
[66]N. Kawakami, Phys. Rev. B **47**, 2928 (1993).
[67]P. Schlottmann, Phys. Rev. B **69**, 035110 (2004).
[68]R. Z. Bariev, A. Klümper, A. Schadschneider, and J. Zittartz, Z. Phys. B **96**, 395 (1995).